Center for Aeronautical Research

Bureau of Engineering Research
The University of Texas at Austin
Austin, Texas

CAR 84-1

A SUBSTRUCTURE COUPLING PROCEDURE APPLICABLE
TO GENERAL LINEAR TIME-INVARIANT
DYNAMIC SYSTEMS

by

Thomas G. Howsman
Roy R. Craig, Jr.

NASA Contract No. NAS8-35338
May, 1984

A SUBSTRUCTURE COUPLING PROCEDURE APPLICABLE

TO GENERAL LINEAR TIME-INVARIANT

DYNAMIC SYSTEMS

A Report to

NASA Marshall Space Flight Center

Contract No. NAS8-35338

by

Thomas G. Howsman*

Roy R. Craig, Jr.+

ASE-EM Department
The University of Texas at Austin
Austin, Texas 78712

*Graduate Student
+Professor, ASE-EM

May, 1984

TABLE OF CONTENTS

Acknowledgement

"Page missing from available version"
5 + 6

Chapter 1

INTRODUCTION

In order to model many of today's complex structural systems, finite element models containing many thousands of degrees of freedom are commonly generated. Often the dimensions of the model are so large that a classical dynamic analysis of the system is computationally impossible, necessitating the use of an alternate method of analysis. Substructure coupling is one such analysis technique employed throughout the aerospace industry.

Over the past several decades a multitude of substructure coupling techniques for undamped structural systems have been developed (Ref. 7), but comparatively few authors have concerned themselves with the coupling of damped systems. Neglecting the velocity terms is often an acceptable approximation for lightly damped structures, but is unacceptable for actively (or passively) controlled systems or for systems which develop Coriolis type forces. The object of this thesis is to present a general substructure coupling procedure applicable to systems possessing general linear damping.

Previous papers pertaining to substructure coupling of damped systems include those by Hasselman and Kaplan, Hale, and Chung. The technique developed by Hasselman and Kaplan (Ref. 14) is an extrapolation of the popular Craig-Bampton method of component mode synthesis for undamped systems. Accordingly, the substructure Ritz vectors used by Hasselman and Kaplan are selected from the set of fixed-interface component modes.

Hale's approach to the damped substructure synthesis problem has been to find an applicable variational principle whose Euler equations are the coupled system equations of motion (Ref. 11). The Ritz vectors employed by Hale to represent each substructure are produced by a variant of subspace iteration.

The coupling procedure presented by Chung has as its basis the Hamiltonian description of the system (Ref. 2). Hamilton's canonical equations are therefore identified as the equations of motion for the system. The substructure Ritz vectors utilized by Chung are a truncated set of free-interface component modes augmented by a set of generalized residual attachment modes.

The substructure coupling procedure to be presented will be valid for systems possessing general nonproportional, even nonsymmetric, damping terms. The coupled system equations of motion will be derived from a variational principle, and free-interface component modes along with a set of attachment modes will serve as the substructure Ritz vectors. The presentation of the method begins in Chapter 2 with the development of the substructure equation of motion. Chapter 3 concerns itself with the substructure interface compatibility conditions. The actual coupling procedure is presented in Chapter 4, and the topic of component Ritz vectors is addressed in Chapter 5. Computational considerations are the subject of Chapter 6. Chapter 7 contains the results of several test problems, and conclusions and recommendations are drawn in Chapter 8. An appendix is provided for those readers unfamiliar with the properties of adjoint differential equations, adjoint eigenproblems, and variational principles.

Chapter 2
DEVELOPMENT OF THE SUBSTRUCTURE EQUATION OF MOTION

For the purposes of this thesis, we will assume that a finite element model of the substructure is available. The equation of motion for each substructure, written in the standard form, is

$$[M]\underset{\sim}{\ddot{x}} + [C]\underset{\sim}{\dot{x}} + [K]\underset{\sim}{x} = \underset{\sim}{f} \qquad (2.1)$$

where $\quad \underset{\sim}{x}$ = displacement vector $\qquad$ [M] = mass matrix

$\qquad\qquad \underset{\sim}{\dot{x}}$ = velocity vector $\qquad$ [C] = damping matrix

$\qquad\qquad \underset{\sim}{\ddot{x}}$ = acceleration vector $\qquad$ [K] = stiffness matrix

The equation of motion, when written in the above form, has several properties worthy of note at this point. First, and perhaps most importantly, Eq. (2.1) does not lend itself to either the standard or generalized eigenproblem form ($\underset{\sim}{A}\underset{\sim}{\phi} = \lambda\underset{\sim}{\phi}$ or $\underset{\sim}{A}\underset{\sim}{\phi} = \lambda\underset{\sim}{B}\underset{\sim}{\phi}$). Another important property of Eq. (2.1) is that it is a non-self-adjoint ordinary differential equation. It may be demonstrated that the differential adjoint of Eq. (2.1) is

$$[M]^T\underset{\sim}{\ddot{y}} - [C]^T\underset{\sim}{\dot{y}} + [K]^T\underset{\sim}{y} = \underset{\sim}{f}^* \qquad (2.2)$$

where $\underset{\sim}{y}$ is the adjoint displacement vector, and $\underset{\sim}{f}^*$ is the adjoint force vector. Inspection of the adjoint equation of motion shows that even if the defining matrices ([M], [C], [K]) are symmetric, which is not assumed, the adjoint operator differs from the original differential operator because of the sign change on the first derivative (damping) term.

9

To cast the equation of motion into a form which leads to a generalized eigenproblem, a state variable substitution will be made. The state variable substitution has the effect of changing the n second-order differential equations into 2n first-order equations.

The transformation of the equation of motion and its adjoint will be accomplished by finding a variational principle which has as its conditions for stationarity (Euler equations) the original differential equations (Ref. 26). The reason for applying a variational principle to the problem at hand is the ease of introducing constraint conditions in a natural manner.

Using the concepts developed in the appendix, it may be seen that the following bilinear functional corresponds to the variational principle associated with Eqs. (2.1) and (2.2):

$$\pi_1 = \int_0^{t_f} \left[\underset{\sim}{y}^T ([M]\ddot{\underset{\sim}{x}} + [C]\dot{\underset{\sim}{x}} + [K]\underset{\sim}{x}) - \underset{\sim}{y}^T \underset{\sim}{f} - \underset{\sim}{x}^T \underset{\sim}{f}^* \right] dt \qquad (2.3)$$

To find the Euler equations of this functional, the first variations of the functional are set to zero, i.e.

$$\int_0^{t_f} \delta \pi_1 \, dt = 0 \qquad (2.4)$$

The above expression can be expanded into the following form:

$$[\text{boundary terms}]_0^{t_f} + \int_0^{t_f} \delta \underset{\sim}{y}^T ([M]\ddot{\underset{\sim}{x}} + [C]\dot{\underset{\sim}{x}} + [K]\underset{\sim}{x} - \underset{\sim}{f}) \, dt$$

$$+ \int_0^{t_f} \delta \underset{\sim}{x}^T ([M]^T \ddot{\underset{\sim}{y}} - [C]^T \dot{\underset{\sim}{y}} + [K]^T \underset{\sim}{y} - \underset{\sim}{f}^*) \, dt = 0 \qquad (2.5)$$

where the boundary terms are the by-products of the integration by parts.

Since variations on the time boundary are disallowed, and variations $\delta \underset{\sim}{y}^T$ and $\delta \underset{\sim}{x}^T$ are arbitrary, the Euler equations for the above expression are seen to be

and
$$[M]\underset{\sim}{\ddot{x}} + [C]\underset{\sim}{\dot{x}} + [K]\underset{\sim}{x} - \underset{\sim}{f} = \underset{\sim}{0} \qquad (2.6a)$$
$$[M]^T\underset{\sim}{\ddot{y}} - [C]^T\underset{\sim}{\dot{y}} + [K]^T\underset{\sim}{y} - \underset{\sim}{f}^* = \underset{\sim}{0} \qquad (2.6b)$$

which are simply the equation of motion and its adjoint.

Up to this point, the equation of motion along with its adjoint have been obtained as the Euler equations of a certain functional, π_1. For reasons discussed earlier, it is desirable to convert the equation of motion into a state vector form. An obvious choice for a state variable substitution is

$$\underset{\sim}{v} = \underset{\sim}{\dot{x}} \qquad (2.7)$$

The above equation is equivalent to

$$[M]\,(\underset{\sim}{\dot{x}} - \underset{\sim}{v}) = \underset{\sim}{0} \qquad (2.8)$$

if the mass matrix is invertible, a condition which will be assumed (Ref. 11). The choice of the mass matrix over other non-singular matrices will be made obvious shortly.

To derive the substructure state vector formulation of the equation of motion, the π_1 functional is modified with the state variable substitution and the appending of the constraint equation to the functional with the use of a Lagrange multiplier vector. The

modified substructure functional, to be called π_2, can be written as

$$\pi_2 = \int_0^{t_f} \left[y^T ([M]\dot{\underset{\sim}{v}} + [C]\dot{\underset{\sim}{x}} + [K]\underset{\sim}{x}) - \underset{\sim}{y}^T\underset{\sim}{f} - \underset{\sim}{x}^T\underset{\sim}{f}^* \right.$$

$$\left. + \underset{\sim}{w}^T[M] (\dot{\underset{\sim}{x}} - \underset{\sim}{v}) \right] dt \tag{2.9}$$

Since there are four vectors of variables ($\underset{\sim}{w}$, $\underset{\sim}{y}$, $\underset{\sim}{v}$, $\underset{\sim}{x}$) to be considered independent in the π_2 functional, there will, of course, be four Euler equations. The four Euler equations are

$$[M]\dot{\underset{\sim}{x}} - [M]\underset{\sim}{v} = \underset{\sim}{0} \tag{2.10a}$$

$$[M]\dot{\underset{\sim}{v}} + [C]\dot{\underset{\sim}{x}} + [K]\underset{\sim}{x} - \underset{\sim}{f} = \underset{\sim}{0} \tag{2.10b}$$

$$-[M]^T\dot{\underset{\sim}{y}} - [M]^T\underset{\sim}{w} = \underset{\sim}{0} \tag{2.10c}$$

$$-[M]^T\dot{\underset{\sim}{w}} - [C]^T\dot{\underset{\sim}{y}} + [K]^T\underset{\sim}{y} - \underset{\sim}{f} = \underset{\sim}{0} \tag{2.10d}$$

These four equations can be conveniently stacked into the following two matrix equations:

$$\begin{bmatrix} [0] & [M] \\ [M] & [C] \end{bmatrix} \begin{Bmatrix} \dot{\underset{\sim}{v}} \\ \dot{\underset{\sim}{x}} \end{Bmatrix} + \begin{bmatrix} -[M] & [0] \\ [0] & [K] \end{bmatrix} \begin{Bmatrix} \underset{\sim}{v} \\ \underset{\sim}{x} \end{Bmatrix} = \begin{Bmatrix} \underset{\sim}{0} \\ \underset{\sim}{f} \end{Bmatrix} \tag{2.11a}$$

$$-\begin{bmatrix} [0] & [M]^T \\ [M]^T & [C]^T \end{bmatrix} \begin{Bmatrix} \dot{\underset{\sim}{w}} \\ \dot{\underset{\sim}{y}} \end{Bmatrix} + \begin{bmatrix} -[M]^T & [0] \\ [0] & [K]^T \end{bmatrix} \begin{Bmatrix} \underset{\sim}{w} \\ \underset{\sim}{y} \end{Bmatrix} = \begin{Bmatrix} \underset{\sim}{0} \\ \underset{\sim}{f}^* \end{Bmatrix} \tag{2.11b}$$

Equation (2.11a) is recognized as the state variable form of the equation of motion (Ref. 3), and Eq. (2.11b) is simply the corresponding differential adjoint equation. This particular form of the equation of motion given in Eq. (2.11a) seems to have been utilized as early as 1946 by Frazer, Duncan, and Collar, who derived it

essentially from considerations of Hamilton's canonical equations of motion (Ref. 8).

An important feature of Eqs. (2.11a) and (2.11b) is the symmetry of the substructure state matrices if the [M], [C], and [K] are symmetric. Hale's formulation of the substructure state variable equation of motion (Ref. 11), although derived by a procedure similar to the one just presented, results in the formation of an unconditionally nonsymmetric substructure state matrix, which is shown in the appendix to be disadvantageous.

If the equation of motion is contrasted with its adjoint, i.e. Eqs. (2.11a) and (2.11b), it is seen that the vector of Lagrange multipliers $\underset{\sim}{w}$ plays the role of the adjoint state velocity. This idea will be utilized when compatibility between substructures is considered.

Writing Eqs. (2.11a) and (2.11b) in a more compact form, we have

$$\underset{\approx}{A}\,\underset{\sim}{\dot{X}} + \underset{\approx}{B}\,\underset{\sim}{X} = \underset{\sim}{F} \qquad (2.12a)$$

$$-\underset{\approx}{A}^{T}\,\underset{\sim}{\dot{Y}} + \underset{\approx}{B}^{T}\,\underset{\sim}{Y} = \underset{\sim}{F}^{*} \qquad (2.12b)$$

where

$$\underset{\approx}{A} = \begin{bmatrix} [0] & [M] \\ [M] & [C] \end{bmatrix} \qquad\qquad \underset{\approx}{B} = \begin{bmatrix} -[M] & [0] \\ [0] & [K] \end{bmatrix}$$

$$(2.13)$$

$$\underset{\sim}{X} = \begin{Bmatrix} \underset{\sim}{v} \\ \underset{\sim}{x} \end{Bmatrix} \qquad\qquad \underset{\sim}{Y} = \begin{Bmatrix} \underset{\sim}{w} \\ \underset{\sim}{y} \end{Bmatrix}$$

As a conclusion to this chapter, the purpose of the mass matrix in Eq. (2.8) will be explored. The mass matrix appears in the state vector equation of motion, and therefore its adjoint, in two locations as a direct result of Eq. (2.8). Referring to the definitions of $\underset{\approx}{A}$ and $\underset{\approx}{B}$ given in Eq. (2.13), the [M] , due to its placement in Eq. (2.8), appears in the upper right quadrant of $\underset{\approx}{A}$, and in the upper left quadrant of $\underset{\approx}{B}$. If the mass matrix used in equation (2.8) is replaced by some other non-singular matrix, the possibility of symmetry in $\underset{\approx}{A}$ is destroyed - a condition to be avoided if possible.

Chapter 3

SYSTEM CONSTRAINTS

3.1   Geometric Compatibility

Consider the adjacent substructures, α and β.
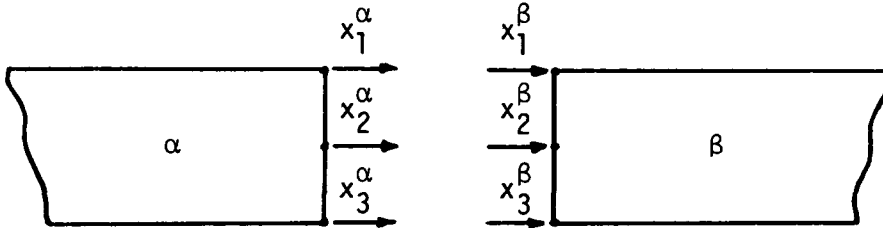
The idea of interface compatibility leads directly to

$$\begin{Bmatrix} x_1 \\ x_2 \\ x_3 \end{Bmatrix}_\alpha = \begin{Bmatrix} x_1 \\ x_2 \\ x_3 \end{Bmatrix}_\beta \tag{3.1}$$

Equation (3.1) simply reflects the fact that the interface displacements of adjacent substructures are identical. This idea will be strictly enforced throughout the coupling procedure. Writing Eq. (3.1) in a more general way, we have

$$\underset{\sim\alpha}{x}^i = \underset{\sim\beta}{x}^i \tag{3.2}$$

where the i denotes interface degrees of freedom.

To obtain the interface degrees of freedom from the arbitrarily arranged displacement vector $\underset{\sim}{x}$, the concept of a "locator" matrix will be employed. This idea is represented by the following equation:

$$\underset{\sim}{x}^i = \underset{\approx 1}{E}\underset{\sim}{x} \tag{3.3}$$

15

If there are i interface degrees of freedom and n total degrees of freedom on the substructure, then the dimensions of $\underset{\approx 1}{E}$ will be i by n. Essentially each row of the locator matrix selects a particular interface coordinate from the substructure displacement vector; hence, each element along the row has a value of zero, except for the element in the column corresponding to the location of the interface coordinate in the $\underset{\sim}{x}$ vector.

If Eq. (3.3) is substituted into Eq. (3.2), the result is

$$(\underset{\sim 1}{E}\underset{\sim}{x})_\alpha = (\underset{\sim 1}{E}\underset{\sim}{x})_\beta \tag{3.4}$$

which will be referred to as the displacement compatibility equation of substructures α and β .

It is clear that the substructure velocities are subject to compatibility across the interface in the same manner as the displacements. However, the necessity of enforcing the velocity constraints is far from clear cut, and there is at least some intuitive evidence supporting both sides of the issue. This evidence will now be reviewed.

The supporting case for mandatory enforcement of the velocity constraints is usually put forth in a heuristic manner. This position has as its basis the physically obvious fact that the velocities are compatible across the interface. Since the velocities are employed as coordinates in the state vector formulation, any constraint condition on them must be included in a viable system functional. This is essentially the argument utilized by Chung in Ref. 2. This argument seems quite logical, or at least intuitively correct, but fails to address several key issues.

When the principles of Lagrangian dynamics are applied to a system containing constraints on displacements (and thereby velocity constraints) only the displacement constraints are appended to the Lagrangian. The velocity constraints certainly exist, but they are not considered in the modified Lagrangian. This situation can be considered somewhat analogous to the substructure coupling problem at hand. It would appear that the constraints on the interface velocities are imposed throughout the system through the state vector substitution

$$\underset{\sim}{v} = \underset{\sim}{\dot{x}} \qquad (3.5)$$

which has already been employed in the substructure equations of motion. In other words, the constraint on the displacements is automatically translated into a constraint on the velocities by Eq. (3.5). Hughes et al. (Ref. 16) have done rather extensive analysis on finite element systems whose displacement and velocity fields are specified independently, and have concluded that the velocity fields do not have to be coupled from element to element. If the substructures to be coupled are considered "superelements," then the analogy between adjacent substructures and adjacent finite elements is clear.

The above concepts form the basis of Hale's position (Ref. 11) that the enforcement of interface velocity compatibility is optional. From a pragmatic point of view, test problems show that it is not necessary to enforce velocity compatibility. However, this is not to say that there are no advantages to enforcing the velocity constraints. There are computational advantages, and these will be considered after the system equations are developed.

To develop the actual form of the velocity compatibility equations, all that is required is the time derivative of Eq. (3.4), i.e.

$$(\underset{\approx}{E}_1 \dot{\underset{\sim}{x}})_\alpha = (\underset{\approx}{E}_1 \dot{\underset{\sim}{x}})_\beta \tag{3.6}$$

The state vector substitution can be applied to the above equation, resulting in the interface velocity compatibility equation

$$(\underset{\approx}{E}_1 \underset{\sim}{v})_\alpha = (\underset{\approx}{E}_1 \underset{\sim}{v})_\beta \tag{3.7}$$

Since the state vector form of the equations of motion will be used almost exclusively throughout the remainder of this thesis, it is desirable to write the above constraint equations in an appropriate form. For example, Eq. (3.4) can be written as

$$[\underset{\approx}{0} \; \vdots \; \underset{\approx}{E}_1] \left\{ \begin{array}{c} \underset{\sim}{v} \\ \hline \underset{\sim}{x} \end{array} \right\} = [\underset{\approx}{0} \; \vdots \; \underset{\approx}{E}_1] \left\{ \begin{array}{c} \underset{\sim}{v} \\ \hline \underset{\sim}{x} \end{array} \right\} \tag{3.8}$$

or

$$\underset{\approx}{E}^x_\alpha \, \underset{\sim}{x}_\alpha = \underset{\approx}{E}^x_\beta \, \underset{\sim}{x}_\beta \tag{3.9}$$

Both the displacement and the velocity constraints, i.e. Eqs. (3.4) and (3.7), can be combined into a single matrix equation in the following way:

$$\begin{bmatrix} \underset{\approx}{E}_1 & \vdots & \underset{\approx}{0} \\ \hline \underset{\approx}{0} & \vdots & \underset{\approx}{E}_1 \end{bmatrix}_\alpha \left\{ \begin{array}{c} \underset{\sim}{v} \\ \hline \underset{\sim}{x} \end{array} \right\}_\alpha = \begin{bmatrix} \underset{\approx}{E}_1 & \vdots & \underset{\approx}{0} \\ \hline \underset{\approx}{0} & \vdots & \underset{\approx}{E}_1 \end{bmatrix}_\beta \left\{ \begin{array}{c} \underset{\sim}{v} \\ \hline \underset{\sim}{x} \end{array} \right\}_\beta \tag{3.10}$$

or

$$\mathbf{\mathop{E}_{\alpha}^{XV}} \; \mathop{X}_{\alpha} = \mathbf{\mathop{E}_{\beta}^{XV}} \; \mathop{X}_{\beta} \qquad\qquad (3.11)$$

An additional topic concerning displacement and velocity compatibility between substructures is the concept of relaxed interface compatibility. If the substructures are represented by a set of partial differential equations, then satisfying the geometric compatibility conditions between substructures in some "average" way is necessary since there are an infinite number of interface degrees of freedom in this representation. Meirovitch and Hale (Refs. 13, 19, 20) have done extensive work in this area, employing a weighted residual approach to satisfy compatibility. These same authors, along with Craig and Chang (Ref. 7), have also examined relaxing the exact geometric compatibility conditions for substructures modeled by ordinary differential equations (finite element models). One effect of relaxing the compatibility conditions is to degrade the accuracy of the computed system eigenvalues. Unfortunately, an a priori estimate of this degradation caused by relaxing the constraints does not exist. Further discussion of approximate compatibility conditions will be postponed until the final form of the coupled system equations of motion has been developed.

3.2   Force Compatibility

Newton's Third Law (action-reaction) provides the key when a relationship between the interface forces is desired. This relationship is obvious when the free-body diagrams of the two adjacent substructures are considered, i.e.
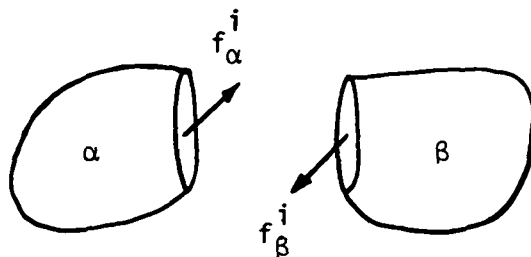
Figure 3.1 Free-Body Diagrams of Adjacent Substructures

As shown in the free-body diagrams, the interface reaction forces are equal in magnitude, but opposite in direction. This is represented by

$$f_\alpha^i + f_\beta^i = 0 \qquad (3.12)$$

which is the equation of substructure interface reaction force compatibility.

As a conclusion to this chapter on compatibility, it should be recognized that the equations of displacement, velocity, and force compatibility developed above are obtained primarily by physical interpretations of the quantities involved. Since the variational procedure employed results in adjoint equations of motion, compatibility equations between these "adjoint substructures" need to be developed. Physically, it is difficult to interpret exactly what the adjoint substructure equations describe, but it seems logical to assume the adjoint compatibility equations will correspond exactly to those of the physical substructures. Hence the adjoint compatibility equations are taken to be

21

$$\underset{\approx}{E}^{X}_{\alpha} \, \underset{\sim}{Y}_{\alpha} = \underset{\approx}{E}^{X}_{\beta} \, \underset{\sim}{Y}_{\beta} \quad , \tag{3.13}$$

$$\underset{\approx}{E}^{XV}_{\alpha} \, \underset{\sim}{Y}_{\alpha} = \underset{\approx}{E}^{XV}_{\beta} \, \underset{\sim}{Y}_{\beta} \, , \tag{3.14}$$

and

$$\underset{\sim}{f}^{*i}_{\alpha} + \underset{\sim}{f}^{*i}_{\beta} = \underset{\sim}{0} \tag{3.15}$$

Chapter 4

DEVELOPMENT OF A SUBSTRUCTURE COUPLING PROCEDURE

In this chapter a general substructure coupling procedure will be developed. Due to the assumed presence of a velocity-dependent term in at least one of the substructure equations of motion, all substructures will be represented in the state vector form (Eq. (2.11)). The basic coupling strategy will now be outlined.

As in the development of the substructure equations of motion, a variational principle will be utilized to obtain the system equations of motion (Ref. 11). The interface compatibility conditions developed in the previous section will be appended to the functional, thereby insuring the satisfaction of compatibility conditions. Finally, a Ritz approximation to the substructure state vector, X , and its adjoint vector, Y , will be incorporated into the functional. The Euler equations for this final form of the system functional will be the coupled system equation of motion, the appropriate constraint equations, and the corresponding adjoint equations.

4.1 The System Functional

Throughout the forthcoming development, it will be assumed that the system under consideration is composed of two substructures, α and β . The developmental details of the system functional are most easily demonstrated when only two substructures exist, but the extrapolation to systems containing many components is straightforward.

Before the system functional is written, the substructure equation of motion and its adjoint will be cast in the following form:

$$A\dot{X} + BX = F^i + F \tag{4.1}$$

and

$$-A^T\dot{Y} + B^T Y = F^{*i} + F^* \tag{4.2}$$

where the force vector has been separated into two parts, the interface reaction forces, F^i and F^{*i}, and all other external forces, F and F^*. It should be noted that F^i is simply f^i augmented with zeros to length 2n. The bilinear substructure functional corresponding to Eqs. (4.1) and (4.2) is

$$\pi_3 = \int_0^t [Y^T (A\dot{X} + BX) - Y^T (F^i + F) - X^T (F^{*i} + F^*)] \; dt \tag{4.3}$$

In order to keep the development general at this point, the geometric compatibility equation to be imposed on the functional will be written as

$$(E\; X)_\alpha - (E\; X)_\beta = 0 \tag{4.4}$$

Note that no superscripts appear on the E matrix in this equation. This is intentional since it is desirable to develop the system equations of motion with, and without, interface velocity compatibility. (See Eqs. (3.9) and (3.11)).

The system functional is simply the sum of the individual substructure functionals plus the appended constraint equations. Hence, the system functional takes the following form:

$$\pi = \pi_3^{\alpha} + \pi_3^{\beta}$$

$$+ \int_0^t \left[\sigma_1^T [(\underset{\approx}{E}\underset{\sim}{X})_\alpha - (\underset{\approx}{E}\underset{\sim}{X})_\beta] + \sigma_2^T [(\underset{\approx}{E}\underset{\sim}{Y})_\alpha - (\underset{\approx}{E}\underset{\sim}{Y})_\beta] \right] dt \tag{4.5}$$

where σ_1^T and σ_2^T are Lagrange multiplier vectors.

If Eq. (4.3) is substituted for π_3^{α} and π_3^{β} in Eq. (4.5), the following expression for the system functional results:

$$\pi = \int_0^t \left[\; (\underset{\sim}{Y}^T [\underset{\approx}{A}\dot{\underset{\sim}{X}} + \underset{\approx}{B}\underset{\sim}{X}] - \underset{\sim}{Y}^T\underset{\sim}{F}^i - \underset{\sim}{Y}^T\underset{\sim}{F} - \underset{\sim}{X}^T\underset{\sim}{F}^{*i} - \underset{\sim}{X}^T\underset{\sim}{F}^{*})_\alpha \right.$$

$$+ \; (\underset{\sim}{Y}^T [\underset{\approx}{A}\dot{\underset{\sim}{X}} + \underset{\approx}{B}\underset{\sim}{X}] - \underset{\sim}{Y}^T\underset{\sim}{F}^i - \underset{\sim}{Y}^T\underset{\sim}{F} - \underset{\sim}{X}^T\underset{\sim}{F}^{*i} - \underset{\sim}{X}^T\underset{\sim}{F}^{*})_\beta \tag{4.6}$$

$$\left. + \; \sigma_1^T [(\underset{\approx}{E}\underset{\sim}{X})_\alpha - (\underset{\approx}{E}\underset{\sim}{X})_\beta] + \sigma_2^T [(\underset{\approx}{E}\underset{\sim}{Y})_\alpha - (\underset{\approx}{E}\underset{\sim}{Y})_\beta] \; \right] dt$$

Upon examination of the terms in the integrand of Eq. (4.6) which contain the interface reaction forces, it becomes clear that only the interface portions of the generalized displacement and force vectors contribute to the inner product. Thus

$$\underset{\sim}{Y}^T\underset{\sim}{F}^i = (\underset{\approx}{E}^X\underset{\sim}{Y})^T (\underset{\approx}{E}^X\underset{\sim}{F}^i) \tag{4.7}$$

where $\underset{\approx}{E}^X$ is defined in Eq. (3.9). Of course, a similar expression exists for the adjoint force terms.

The purpose of isolating the interface reaction forces from the external forces in Eqs. (4.1) and (4.2) will now be made apparent. The

interface reaction force terms of the system functional can be combined with Eq. (4.7) to yield

$$-(\underset{\sim}{Y}^T \underset{\sim}{F}^i)_\alpha - (\underset{\sim}{Y}^T \underset{\sim}{F}^i)_\beta - (\underset{\sim}{X}^T \underset{\sim}{F}^{*i})_\alpha - (\underset{\sim}{X}^T \underset{\sim}{F}^{*i})_\beta =$$

$$-(\underset{\approx}{E}^X \underset{\sim}{Y})_\alpha^T (\underset{\approx}{E}^X \underset{\sim}{F}^i)_\alpha - (\underset{\approx}{E}^X \underset{\sim}{Y})_\beta^T (\underset{\approx}{E}^X \underset{\sim}{F}^i)_\beta - (\underset{\approx}{E}^X \underset{\sim}{X})_\alpha^T (\underset{\approx}{E}^X \underset{\sim}{F}^{*i})_\alpha \qquad (4.8)$$

$$- (\underset{\approx}{E}^X \underset{\sim}{X})_\beta^T (\underset{\approx}{E}^X \underset{\sim}{F}^{*i})_\beta$$

Since $\underset{\approx}{E}^X \underset{\sim}{F}^i$ is equivalent to $\underset{\sim}{f}^i$, Eq. (4.8) can be combined with the interface reaction force compatibility equation (i.e. Eq. (3.12)) to yield

$$-(\underset{\sim}{Y}^T \underset{\sim}{F}^i)_\alpha - (\underset{\sim}{Y}^T \underset{\sim}{F}^i)_\beta - (\underset{\sim}{X}^T \underset{\sim}{F}^{*i})_\alpha - (\underset{\sim}{X}^T \underset{\sim}{F}^{*i})_\beta =$$

$$-[(\underset{\approx}{E}^X \underset{\sim}{Y})_\alpha^T - (\underset{\approx}{E}^X \underset{\sim}{Y})_\beta^T] \, \underset{\sim}{f}^i - [(\underset{\approx}{E}^X \underset{\sim}{X})_\alpha^T - (\underset{\approx}{E}^X \underset{\sim}{X})_\beta^T] \, \underset{\sim}{f}^{*i} \qquad (4.9)$$

As mentioned previously, interface displacement compatibility will be strictly enforced throughout the coupling procedure. This fact, represented by Eq. (4.4), immediately allows us to conclude that the right hand side of Eq. (4.9) vanishes, hence

$$-(\underset{\sim}{Y}^T \underset{\sim}{F}^i)_\alpha - (\underset{\sim}{Y}^T \underset{\sim}{F}^i)_\beta - (\underset{\sim}{X}^T \underset{\sim}{F}^{*i})_\alpha - (\underset{\sim}{X}^T \underset{\sim}{F}^{*i})_\beta = 0 \qquad (4.10)$$

Equation (4.10) can be combined with Eq. (4.6), resulting in the following form of the system functional:

$$\pi = \int_0^t \Big[\ (\underset{\sim}{Y}^T [\underset{\approx}{A}\dot{\underset{\sim}{X}} + \underset{\approx}{B}\underset{\sim}{X}] - \underset{\sim}{Y}^T \underset{\sim}{F} - \underset{\sim}{X}^T \underset{\sim}{F}^*)_\alpha$$

$$+ \ (\underset{\sim}{Y}^T [\underset{\approx}{A}\underset{\sim}{X} + \underset{\approx}{B}\underset{\sim}{X}] - \underset{\sim}{Y}^T \underset{\sim}{F} - \underset{\sim}{X}^T \underset{\sim}{F}^*)_\beta \qquad (4.11)$$

$$+ \ \underset{\sim}{\sigma}_1^T [(\underset{\approx}{E}\underset{\sim}{X})_\alpha - (\underset{\approx}{E}\underset{\sim}{X})_\beta] + \underset{\sim}{\sigma}_2^T [(\underset{\approx}{E}\underset{\sim}{Y})_\alpha - (\underset{\approx}{E}\underset{\sim}{Y})_\beta] \ \Big] \ dt$$

Notice that the interface reaction force terms no longer exist in the system functional.

4.2   Introduction of Ritz Vectors

In order to implement a reduced-order system model, a Ritz vector approximation to the substructure generalized displacement field (i.e. state vectors $\underset{\sim}{X}$ and $\underset{\sim}{Y}$) will be incorporated in the system functional. The form of this approximation is as follows:

$$\underset{\sim}{X} = \sum_{j=1}^{N_x} \underset{\sim}{\phi}_{xj} \, \eta_{xj} = \underset{\approx}{\Phi}_x \, \underset{\sim}{\eta}_x \tag{4.12}$$

and

$$\underset{\sim}{Y} = \sum_{j=1}^{N_y} \underset{\sim}{\phi}_{yj} \, \eta_{yj} = \underset{\approx}{\Phi}_y \, \underset{\sim}{\eta}_y \tag{4.13}$$

where $\underset{\approx}{\Phi}$ is the matrix of Ritz vectors and $\underset{\sim}{\eta}$ is the vector of the time-dependent generalized coordinates. Of course, the number of Ritz vectors used in the approximation must not be larger than the total number of substructure degrees of freedom, i.e.

$$N_x, N_y \leq 2n \tag{4.14}$$

The approximate system functional is formed by substituting the Ritz approximations into the previous expression for the system functional. This new functional takes the form

$$\pi_a = \int_0^t (\underset{\sim}{n}_y^T \underset{\sim}{\phi}_y^T [\underset{\approx}{A}\underset{\sim}{\phi}_x \underset{\sim}{n}_x + \underset{\approx}{B}\underset{\sim}{\phi}_x \underset{\sim}{n}_x] - \underset{\sim}{n}_y^T \underset{\sim}{\phi}_y^T \underset{\sim}{F} - \underset{\sim}{n}_x^T \underset{\sim}{\phi}_x \underset{\sim}{F}^*)_\alpha$$

$$+ (\underset{\sim}{n}_y^T \underset{\sim}{\phi}_y^T [\underset{\approx}{A}\underset{\sim}{\phi}_x \underset{\sim}{n}_x + \underset{\approx}{B}\underset{\sim}{\phi}_x \underset{\sim}{n}_x] - \underset{\sim}{n}_y^T \underset{\sim}{\phi}_y^T \underset{\sim}{F} - \underset{\sim}{n}_x \underset{\sim}{\phi}_x \underset{\sim}{F}^*)_\beta \qquad (4.15)$$

$$+ \underset{\sim}{\sigma}_1^T [(\underset{\approx}{E}\underset{\sim}{\phi}_x \underset{\sim}{n}_x)_\alpha - (\underset{\approx}{E}\underset{\sim}{\phi}_x \underset{\sim}{n}_x)_\beta] + \underset{\sim}{\sigma}_2^T [(\underset{\approx}{E}\underset{\sim}{\phi}_y \underset{\sim}{n}_y)_\alpha - (\underset{\approx}{E}\underset{\sim}{\phi}_y \underset{\sim}{n}_y)_\beta] \qquad dt$$

The actual form of the Ritz vectors will be discussed in a subsequent chapter.

4.3   The System Equations

The Euler equations of the approximate system functional are the system equations of motion as well as the appropriate constraint equations. In order to insure stationarity of π_a , six quantities must be varied - $\underset{\sim}{n}_{y\alpha}^T$, $\underset{\sim}{n}_{x\alpha}^T$, $\underset{\sim}{n}_{y\beta}^T$, $\underset{\sim}{n}_{x\beta}^T$, $\underset{\sim}{\sigma}_1^T$, and $\underset{\sim}{\sigma}_2^T$. Hence the approximate system functional will produce six Euler equations. These Euler equations are easily shown to be

$$(\underset{\sim}{\phi}_y^T \underset{\approx}{A} \underset{\sim}{\phi}_x \dot{\underset{\sim}{n}}_x)_\alpha + (\underset{\sim}{\phi}_y^T \underset{\approx}{B} \underset{\sim}{\phi}_x \underset{\sim}{n}_x)_\alpha = (\underset{\sim}{\phi}_y^T \underset{\sim}{F})_\alpha - (\underset{\sim}{\phi}_y^T \underset{\approx}{E}^T)_\alpha \underset{\sim}{\sigma}_2 \qquad (4.16a)$$

$$(\underset{\sim}{\phi}_y^T \underset{\approx}{A} \underset{\sim}{\phi}_x \dot{\underset{\sim}{n}}_x)_\beta + (\underset{\sim}{\phi}_y^T \underset{\approx}{B} \underset{\sim}{\phi}_x \underset{\sim}{n}_x)_\beta = (\underset{\sim}{\phi}_y^T \underset{\sim}{F})_\beta + (\underset{\sim}{\phi}_y^T \underset{\approx}{E}^T)_\beta \underset{\sim}{\sigma}_2 \qquad (4.16b)$$

$$-(\underset{\sim}{\phi}_x^T \underset{\approx}{A}^T \underset{\sim}{\phi}_y \dot{\underset{\sim}{n}}_y)_\alpha + (\underset{\sim}{\phi}_x^T \underset{\approx}{B}^T \underset{\sim}{\phi}_y \underset{\sim}{n}_y)_\alpha = (\underset{\sim}{\phi}_x^T \underset{\sim}{F}^*)_\alpha - (\underset{\sim}{\phi}_x^T \underset{\approx}{E}^T)_\alpha \underset{\sim}{\sigma}_1 \qquad (4.16c)$$

$$-(\underset{\sim}{\phi}_x^T \underset{\approx}{A}^T \underset{\sim}{\phi}_y \dot{\underset{\sim}{n}}_y)_\beta + (\underset{\sim}{\phi}_x^T \underset{\approx}{B}^T \underset{\sim}{\phi}_y \underset{\sim}{n}_y)_\beta = (\underset{\sim}{\phi}_x^T \underset{\sim}{F}^*)_\beta + (\underset{\sim}{\phi}_x^T \underset{\approx}{E}^T)_\beta \underset{\sim}{\sigma}_1 \qquad (4.16d)$$

$$(\underset{\approx}{E} \underset{\sim}{\phi}_x \underset{\sim}{n}_x)_\alpha - (\underset{\approx}{E} \underset{\sim}{\phi}_x \underset{\sim}{n}_x)_\beta = \underset{\sim}{0} \qquad (4.16e)$$

$$(\underset{\approx}{E} \underset{\sim}{\phi}_y \underset{\sim}{n}_y)_\alpha - (\underset{\approx}{E} \underset{\sim}{\phi}_y \underset{\sim}{n}_y)_\beta = \underset{\sim}{0} \qquad (4.16f)$$

Clearly Eqs. (4.16a), (4.16b), and (4.16e) relate to the system equations of motion, whereas Eqs. (4.16c), (4.16d), and (4.16f) pertain to the adjoint system equations of motion. Equations (4.16a) and (4.16b) are equivalent to the following matrix equation:

$$
\begin{bmatrix} \Phi_{y\alpha} & 0 \\ 0 & \Phi_{y\beta} \end{bmatrix}^T
\begin{bmatrix} A_\alpha & 0 \\ 0 & A_\beta \end{bmatrix}
\begin{bmatrix} \Phi_{x\alpha} & 0 \\ 0 & \Phi_{x\beta} \end{bmatrix}
\begin{Bmatrix} \dot{\eta}_{x\alpha} \\ \dot{\eta}_{x\beta} \end{Bmatrix} +
$$

$$
\begin{bmatrix} \Phi_{y\alpha} & 0 \\ 0 & \Phi_{y\beta} \end{bmatrix}^T
\begin{bmatrix} B_\alpha & 0 \\ 0 & B_\beta \end{bmatrix}
\begin{bmatrix} \Phi_{x\alpha} & 0 \\ 0 & \Phi_{x\beta} \end{bmatrix}
\begin{Bmatrix} \eta_{x\alpha} \\ \eta_{x\beta} \end{Bmatrix} = \qquad (4.17)
$$

$$
\begin{bmatrix} \Phi_{y\alpha} & 0 \\ 0 & \Phi_{y\beta} \end{bmatrix}^T
\begin{Bmatrix} F_\alpha \\ F_\beta \end{Bmatrix}
+ \; [-E\,\Phi_{y\alpha} \; \vdots \; E\Phi_{y\beta}]^T \; \sigma_2
$$

or in abbreviated form

$$
\Phi_y^T \, A_{bk} \, \Phi_x \, \dot{\eta} \;\; + \;\; \Phi_y^T \, B_{bk} \, \Phi_x \, \dot{\eta}
$$

$$
= \;\; \Phi_y^T \, F \;\; + \;\; [-E\Phi_{y\alpha} \quad E\Phi_{y\beta}]^T \, \sigma_2 \qquad (4.18)
$$

where Φ_y , Φ_x , A_{bk} , B_{bk} are simply the block-diagonal matrices represented in Eq. (4.17).

At this point, the equations of motion for each substructure have yet to be coupled in their final form. Indeed, the system equation represented by Eq. (4.17) is coupled only by the unknown vector of Lagrange multipliers (σ_2), which can be directly related to the substructure interface reaction forces. The system equation of motion cannot be solved until σ_2 is in someway eliminated. The

elimination of $\underset{\sim}{\sigma}_2$ will be achieved by applying the constraint equations to Eq. (4.18).

Equations (4.16e) and (4.16f) can be cast in the following convenient forms:

$$[(\underset{\approx}{E}\underset{\approx}{\Phi}_x)_\alpha \quad (-\underset{\approx}{E}\underset{\approx}{\Phi}_x)_\beta] \begin{Bmatrix} \underset{\sim}{\eta}_{x\alpha} \\ \\ \underset{\sim}{\eta}_{x\beta} \end{Bmatrix} = \underset{\sim}{0} \tag{4.19}$$

and

$$[(\underset{\approx}{E}\underset{\approx}{\Phi}_y)_\alpha \quad (-\underset{\approx}{E}\underset{\approx}{\Phi}_y)_\beta] \begin{Bmatrix} \underset{\sim}{\eta}_{y\alpha} \\ \\ \underset{\sim}{\eta}_{y\beta} \end{Bmatrix} = \underset{\sim}{0} \tag{4.20}$$

By their very existence, the constraint equations imply that not all of the substructure generalized coordinates (η's) are independent. If Eqs. (4.19) and (4.20) are partitioned into user-defined dependent and independent coordinates, the following two equations result:

$$[(\underset{\approx}{E}\underset{\approx}{\Phi}_x)_I \quad (\underset{\approx}{E}\underset{\approx}{\Phi}_x)_D] \begin{Bmatrix} \underset{\sim}{\eta}_{xI} \\ \\ \underset{\sim}{\eta}_{xD} \end{Bmatrix} = \underset{\sim}{0} \tag{4.21}$$

and

$$[(\underset{\approx}{E}\underset{\approx}{\Phi}_y)_I \quad (\underset{\approx}{E}\underset{\approx}{\Phi}_y)_D] \begin{Bmatrix} \underset{\sim}{\eta}_{yI} \\ \\ \underset{\sim}{\eta}_{yD} \end{Bmatrix} = \underset{\sim}{0} \tag{4.22}$$

where the number of dependent coordinates is equal to the number of constraint equations to be enforced.

Manipulation of Eq. (4.21) yields

$$\underset{\sim}{\eta}_{xD} = -(\underset{\approx\approx}{E\Phi}_x)_D^{-1} (\underset{\approx\approx}{E\Phi}_x)_I \ \underset{\sim}{\eta}_{xI} \qquad (4.23)$$

which leads directly to the following transformation:

$$\begin{Bmatrix} \underset{\sim}{\eta}_{xI} \\[2mm] \underset{\sim}{\eta}_{xD} \end{Bmatrix} = \begin{bmatrix} \underset{\approx}{I}_I \\ \rule{4cm}{0.4pt} \\ -(\underset{\approx\approx}{E\Phi}_x)_D^{-1} \quad (\underset{\approx\approx}{E\Phi}_x)_I \end{bmatrix} \underset{\sim}{\eta}_{xI} \qquad (4.24)$$

A similar transformation of the adjoint coordinates is

$$\begin{Bmatrix} \underset{\sim}{\eta}_{yI} \\[2mm] \underset{\sim}{\eta}_{yD} \end{Bmatrix} = \begin{bmatrix} \underset{\approx}{I}_I \\ \rule{4cm}{0.4pt} \\ -(\underset{\approx\approx}{E\Phi}_y)_D^{-1} \quad (\underset{\approx\approx}{E\Phi}_y)_I \end{bmatrix} \underset{\sim}{\eta}_{yI} \qquad (4.25)$$

The transformation matrices used in Eqs. (4.24) and (4.25) will be designated as $\underset{\approx}{C}_x$ and $\underset{\approx}{C}_y$ respectively.

A characteristic of the above transformation matrices, whose importance will be demonstrated shortly, is the following matrix identity:

$$[(\underset{\approx\approx}{E\Phi}_x)_I \ (\underset{\approx\approx}{E\Phi}_x)_D] \ \underset{\approx}{C}_x$$

$$= [(\underset{\approx\approx}{E\Phi}_x)_I \ (\underset{\approx\approx}{E\Phi}_x)_D] \begin{bmatrix} \underset{\approx}{I}_I \\ \rule{4cm}{0.4pt} \\ -(\underset{\approx\approx}{E\Phi}_x)_D^{-1} \quad (\underset{\approx\approx}{E\Phi}_x)_I \end{bmatrix} = \underset{\approx}{0} \qquad (4.26)$$

Naturally, an equivalent adjoint identity exists.

If Eq. (4.24) is substituted into Eq. (4.18), and the result premultiplied by $\underset{\sim}{C_y}^T$, the following form of the system equation of motion results:

$$\underset{\sim}{C_y}^T \underset{\sim}{\Phi_y}^T \underset{\approx}{A_{bk}} \underset{\sim}{\Phi_x} \underset{\sim}{C_x} \underset{\sim}{\dot{n}}_{xI} + \underset{\sim}{C_y}^T \underset{\sim}{\Phi_y}^T \underset{\approx}{B_{bk}} \underset{\sim}{\Phi_x} \underset{\sim}{C_x} \underset{\sim}{\dot{n}}_{xI} =$$

$$(4.27)$$

$$\underset{\sim}{C_y}^T \underset{\sim}{\Phi_y}^T \underset{\sim}{F} + \underset{\sim}{C_y}^T [(\underset{\approx}{E}\underset{\sim}{\Phi_y})_I \ (\underset{\approx}{E}\underset{\sim}{\Phi_y})_D] \ \underset{\sim}{\sigma_2}$$

In the formulation of the above equation, it has been implicitly assumed that the substructure Ritz vectors have been arranged in such a manner as to be compatible with the arrangements in Eqs. (4.21) and (4.22).

The last term in Eq. (4.27) is seen to be the transpose of the adjoint version of Eq. (4.26); therefore, the coefficient matrix of the unknown Lagrange multiplier vector vanishes. The system equation of motion is now allowed to take its final form,

$$\underset{\approx}{A}_{sys} \underset{\sim}{\dot{n}}_{sys} + \underset{\approx}{B}_{sys} \underset{\sim}{n}_{sys} = \underset{\sim}{F}_{sys} \qquad (4.28)$$

where

$$\underset{\approx}{A}_{sys} = \underset{\sim}{C_y}^T \underset{\sim}{\Phi_y}^T \underset{\approx}{A}_{bk} \underset{\sim}{\Phi_x} \underset{\sim}{C_x}$$

$$\underset{\approx}{B}_{sys} = \underset{\approx}{C_y}^T \underset{\approx}{\Phi_y}^T \underset{\approx}{B}_{bk} \underset{\approx}{\Phi_x} \underset{\approx}{C_x}$$

and

$$\underset{\sim}{F}_{sys} = \underset{\approx}{C_y}^T \underset{\approx}{\Phi_y}^T \underset{\sim}{F}$$

A system adjoint equation of motion can be formed in a manner paralleling the development of Eq. (4.28), but in practice the adjoint system equation appears to be of little interest in the analysis of the coupled system. This is not to imply that the adjoint equations which appear throughout the development of the coupling procedure are mere mathematical by-products of the variational principles employed. Indeed, the use of adjoint operators is central to the concept of a variational principle for non-self-adjoint operators such as those which describe the motion of generally damped systems (Ref. 9).

Chapter 5

COMPONENT RITZ VECTORS

As mentioned in the previous chapter, the coupling procedure being developed involves a Ritz approximation to the substructure displacement and velocity fields. The only requirements that the Ritz vectors must satisfy are that they be independent and that they satisfy the kinematic boundary conditions of the substructure. Of course, the more accurately the Ritz vectors approximate the actual motion of the substructure, the more accurate the final coupled system will be modeled.

Throughout the evolution of substructure coupling techniques, the formation and selection of component Ritz vectors has been a topic of much investigation, and justifiably so. The less computational effort spent defining the component Ritz vectors, the "cheaper" the overall coupling procedure. The vast majority of substructure coupling techniques employ a truncated set of component modes along with a set of static displacement vectors as the component Ritz vectors, hence the term "component mode synthesis." This is not to say that opponents of the use of component modes as Ritz vectors do not exist, for they do. This school of thought is probably best represented by Hale and Meirovitch, who advocate the use of "admissible vectors" as the component Ritz vectors (Ref. 19). These "admissible vectors" have been obtained in several ways, ranging in sophistication from finite element shape functions to variants of subspace iteration. Unfortunately, a formal proof that the use of admissible vectors in lieu of component

modes leads to comparable accuracy with less computational effort has yet to be demonstrated.

For the coupling procedure being developed, a truncated set of substructure modes augmented by a set of attachment modes will be employed as the substructure Ritz vectors. The reason behind this particular choice of Ritz vectors is basically two-fold - first, the relative ease of obtaining these particular types of Ritz vectors, and second, the proven accuracy of methods employing normal and attachment modes for undamped systems (Ref. 7).

It is clear from Eq. (4.28) that the standard and the adjoint Ritz vectors play equally important roles in the system equation of motion. Considerable computational effort will be saved if the two classes of Ritz vectors are chosen to be identical, i.e.

$$\underset{\approx}{\Phi}_y = \underset{\approx}{\Phi}_x \qquad (5.1)$$

Additionally, a practical consideration favoring the use of the standard eigenvectors as both types of Ritz vectors is the fact that the standard eigenvectors can be measured experimentally. The adjoint eigenvectors, however, are much more elusive, presently evading even a heuristic physical interpretation.

The assumption implied by Eq. (5.1) is quite acceptable since the conditions that the standard Ritz vectors must satisfy are identical to the conditions required of the adjoint Ritz vectors (Ref. 11). Definitions of the particular Ritz vectors to be employed will now be presented.

5.1   Substructure Modes

Previously it was noted that in order to form the substructure eigenproblem a state vector formulation was necessary. This state vector equation of motion was shown to have the form

$$\underset{\approx}{A}\dot{\underset{\sim}{X}} + \underset{\approx}{B}\underset{\sim}{X} = \underset{\sim}{F} \tag{5.2}$$

where $\underset{\approx}{A}$, $\underset{\approx}{B}$, $\underset{\sim}{F}$, and $\underset{\sim}{X}$ are defined in Eq. (2.13). Since the coupling procedure deals exclusively with state vector equations, the term "substructure mode" will be equated with the eigenvectors of the homogeneous form of Eq. (5.2).

When calculating the substructure eigenvectors, the substructures are to be considered completely disjoint (i.e. totally isolated from one another). Hence the eigenvectors that are formed are the free-interface modes. These modes are obtained by substituting $\underset{\sim}{X} = \underset{\sim}{\psi}_X e^{\lambda t}$ into the homogeneous state vector equation of motion, i.e.

$$\lambda \underset{\approx}{A}\underset{\sim}{\psi}_X + \underset{\approx}{B}\underset{\sim}{\psi}_X = \underset{\sim}{0} \tag{5.3a}$$

Equation (5.3a) is recognized as a generalized eigenproblem, and can be readily solved by a number of algorithms. Generally the eigenvectors obtained from Eq. (5.3a) are complex, and commonly come in complex conjugate pairs.

Logically, an adjoint eigenproblem corresponding to the adjoint equation of motion can be formulated. This eigenproblem is shown in the appendix to have the form

$$\lambda \underset{\approx}{A}^T\underset{\sim}{\psi}_y + \underset{\approx}{B}^T\underset{\sim}{\psi}_y = \underset{\sim}{0} \tag{5.3b}$$

It should be repeated that the adjoint (left-hand) eigenvectors are not used as adjoint Ritz vectors, since Eq. (5.1) stipulates that the adjoint Ritz vectors are taken to be identical to the standard Ritz vectors. Accordingly, the standard eigenvectors serve as both standard and adjoint Ritz vectors, as mentioned previously.

If desired, the substructure standard eigenproblem can be obtained from Eq. (5.3a) by multiplying through by $\underset{\approx}{A}^{-1}$. This results in

$$\lambda \underset{\sim}{\psi}_X + \underset{\approx}{A}^{-1} \underset{\approx}{B} \underset{\sim}{\psi}_X = \underset{\sim}{0} \qquad (5.4)$$

which is recognized as a standard eigenproblem. Of course, if $\underset{\approx}{A}^{-1}$ does not exist, the substructure eigenproblem must be formulated in the generalized form.

Upon inspection of the $\underset{\approx}{A}$ matrix, $\underset{\approx}{A}^{-1}$ is seen to have ,the form

$$\underset{\approx}{A} = \begin{bmatrix} [0] & [M] \\ [M] & [C] \end{bmatrix} \qquad \underset{\approx}{A}^{-1} = \begin{bmatrix} -[M]^{-1}[C][M]^{-1} & [M]^{-1} \\ [M]^{-1} & [0] \end{bmatrix} \qquad (5.5a,b)$$

The expression for $\underset{\approx}{A}^{-1}$ clearly shows that the condition that governs the existence of $\underset{\approx}{A}^{-1}$ is the existence of $[M]^{-1}$.

Although the existence of $\underset{\approx}{A}^{-1}$ is necessary for the development of the standard eigenproblem, in practice the computation of $\underset{\approx}{A}^{-1}$ is rather inefficient and is usually replaced by one of several numerical procedures, primarily the Cholesky decomposition of $\underset{\approx}{A}$ (Ref. 1).

As a conclusion to the topic of substructure modes, a discussion of substructure rigid-body modes will be presented. Naturally

an unrestrained substructure will possess rigid-body modes, but some question arises as to how these rigid-body modes manifest themselves in a state vector formulation. From the standard formulation of the substructure equation of motion (Eq. (2.1)), the substructure rigid-body modes can be defined by

$$[K]\underset{\sim}{x} = \underset{\sim}{0} \tag{5.6}$$

where [K] is the singular stiffness matrix.

If Eq. (5.6) defines the rigid-body modes with respect to the displacement coordinates, then the time derivative of Eq. (5.6) should lead to the rigid-body modes defined on the velocity coordinates (Ref.2). Since $\underset{\sim}{\dot{x}} = \underset{\sim}{v}$,

$$[K]\underset{\sim}{\dot{x}} = \underset{\sim}{0} \tag{5.7}$$

is equivalent to

$$[K]\underset{\sim}{v} = \underset{\sim}{0} \tag{5.8}$$

It should be noted that the actual mode shapes generated by equations (5.6) and (5.8) are identical, hence the substructure state vector rigid-body mode set can be defined as

$$\underset{\approx}{\psi}_{RB} = \begin{bmatrix} \underset{\approx}{\phi}_{RB} & \vdots & \underset{\approx}{0} \\ \hdashline & \vdots & \\ \underset{\approx}{0} & \vdots & \underset{\approx}{\phi}_{RB} \end{bmatrix} \tag{5.9}$$

where $\underset{\approx}{\phi}_{RB}$ are the rigid-body mode shapes calculated from either Eq. (5.6) or (5.8). The structure of the $\underset{\approx}{\psi}_{RB}$ matrix adheres to the

concept of independently specified displacement and velocity fields (Ref. 16). Also, the dimensions of $\underset{\approx RB}{\psi}$ satisfy the intuitive notion that the number of rigid-body "modes" in the state vector formulation should be twice the number of rigid-body modes in the displacement formulation.

A pertinent question at this point would be to ask why the rigid-body modes produced by the particular eigensolver employed to find the flexible modes discussed earlier should be replaced by the rigid-body modes defined in Eq. (5.9). In some cases, depending on what type of eigensolver is employed, the $\underset{\approx RB}{\phi}$ shapes may indeed be produced correctly by the eigensolver. Unfortunately, many times the $\underset{\approx RB}{\phi}$ shapes are returned with distortion due to the very iteration process that created them (Ref. 21). It appears that the convergence tolerance which is quite acceptable for the flexible modes fails, in some instances, to provide accurate rigid-body mode shapes in the state vector form. Hence the need for an alternate formulation of the rigid-body mode shapes.

5.2   Attachment Modes

As stated previously, the coupling procedure being developed will employ a truncated set of substructure free-interface modes along with a set of attachment modes as the substructure Ritz vectors. Intuitively it is clear that if the entire set of substructure modes is identified as the set of Ritz vectors, then the entire "motion space" of the substructure will be spanned by the Ritz vectors. Since a reduced-order system model is desired, only a portion of substructure modes will be used; hence the motion space will not be completely

spanned. Restricting the motion space of the substructure has the effect of making the substructure appear stiffer than it really is. Said another way, the substructure has lost the flexibility represented by the discarded modes. Chung has shown by examples that if the substructure is represented only by a truncated set of low frequency modes, the accuracy of the system eigenvalues is rather poor (Ref. 2). It will be seen that if the low frequency modes are augmented by a set of static displacement vectors, to be called attachment modes, the accuracy of the system eigenvalues is significantly improved. This improvement is due to the fact that, in general, the attachment modes implicitly contain the high frequency modes which were truncated. When the attachment modes are included as Ritz vectors, part of the flexibility that they impart to the substructure is due to the implicit presence of the high frequency modes.

In its most basic form, an attachment mode can be defined as the deflection shape the substructure takes on due to a unit load at an interface degree of freedom, i.e.

$$[K] \, \underset{\approx}{\Phi}_A \; = \; \underset{\approx}{F} \qquad\qquad (5.10)$$

where $[K]$ is the substructure stiffness matrix

$\underset{\approx}{\Phi}_A$ is the matrix whose columns are the attachment modes

$\underset{\approx}{F}$ is the matrix of unit interface forces

If the substructure is restrained against rigid-body motion, the attachment modes are seen to be simply the columns of the flexibility matrix which correspond to the interface degrees of freedom.

To this point, the discussion of the attachment modes has only dealt with the displacement portion of the state vector. The velocity coordinates which make up the rest of the state vector will be set to zero since, as stated previously, the attachment modes are derived as the static responses to unit interface loads.

The block-diagonal nature of $\underset{\approx}{B}$ lends itself nicely to definition of the standard attachment modes defined in Eq. (5.10). By inspection, $\underset{\approx}{B}^{-1}$ is seen to be

$$\underset{\approx}{B}^{-1} = \begin{bmatrix} -[M]^{-1} & [0] \\ [0] & [K]^{-1} \end{bmatrix} \tag{5.11}$$

assuming $[M]^{-1}$ and $[K]^{-1}$ exist. It is apparent that the column vectors of $\underset{\approx}{B}^{-1}$ which correspond to the displacement interface degrees of freedom have zero velocity portions. Hence, the standard state vector attachment modes are recognized as columns of generalized flexibility matrix, $\underset{\approx}{B}^{-1}$.

If the contribution of the kept low-frequency modes is removed from the attachment modes, thereby insuring independence of all Ritz vectors, the so-called "residual attachment modes" are formed. In other words, if the attachment modes developed from Eq. (5.10) are expressed in a modal expansion, only the portion due to the discarded high frequency modes will be utilized as residual attachment modes.

Just as the standard attachment modes are defined as columns of the flexibility matrix, $[K]^{-1}$, or more precisely the generalized flexibility matrix, $\underset{\approx}{B}^{-1}$, the residual attachment modes can be defined from the generalized residual flexibility matrix. The residual

flexibility matrix for the non-self-adjoint problem at hand will now be developed.

The generalized pseudo-static response problem for the substructure can be written as

$$\underset{\sim}{B}\underset{\sim}{X} = \underset{\sim}{F} \tag{5.12}$$

The generalized displacement state vector can be expanded in terms of the standard right-hand eigenvectors of the substructure, i.e.

$$\underset{\sim}{X} = \sum_{i=1}^{2n} \underset{\sim}{\psi}_{iR} \, \rho_i = \underset{\approx}{\Psi}_R \, \underset{\sim}{\rho} \tag{5.13}$$

where $\underset{\approx}{\Psi}_R$ is simply the set of eigenvectors obtained from Eq. (5.3a). If Eq. (5.13) is substituted into Eq. (5.12), then the result premultiplied by the set of left-hand (adjoint) substructure eigenvectors yields

$$\underset{\approx}{\Psi}_L^T \, \underset{\approx}{B} \, \underset{\approx}{\Psi}_R \, \underset{\sim}{\rho} = \underset{\approx}{\Psi}_L^T \, \underset{\sim}{F} \tag{5.14}$$

where the adjoint eigenvectors $(\underset{\approx}{\Psi}_L^T)$ are obtained from Eq. (5.3b). The property of bi-orthonormality, developed in the appendix, allows Eq. (5.14) to be written as

$$- \left[\ddots \lambda \ddots \right] \underset{\sim}{\rho} = \underset{\approx}{\Psi}_L^T \, \underset{\sim}{F} \tag{5.15}$$

or

$$\underset{\sim}{\rho} = - \left[\ddots \frac{1}{\lambda} \ddots \right] \underset{\approx}{\Psi}_L^T \, \underset{\sim}{F} \tag{5.16}$$

where the λ's are the substructure eigenvalues. Substitution of Eq. (5.16) back into Eq. (5.13) produces the following form of the generalized displacement vector

$$\underset{\sim}{X} = -\underset{\approx}{\Psi}_R \left[\frac{1}{\lambda} \right] \underset{\approx}{\Psi}_L^T \underset{\sim}{F} \tag{5.17}$$

Upon examination of Eqs. (5.12) and (5.17), it becomes clear that

$$\underset{\approx}{B}^{-1} = -\underset{\approx}{\Psi}_R \left[\frac{1}{\lambda} \right] \underset{\approx}{\Psi}_L^T \tag{5.18}$$

The right-hand side of Eq. (5.18) can be written as a summation, i.e.

$$\underset{\approx}{B}^{-1} = \sum_{i=1}^{2n} \frac{\underset{\sim}{\psi}_{iR} \underset{\sim}{\psi}_{iL}^T}{-\lambda_i} \tag{5.19a}$$

or

$$\underset{\approx}{B}^{-1} = \sum_{i=1}^{n_k} \frac{\underset{\sim}{\psi}_{iR} \underset{\sim}{\psi}_{iL}^T}{-\lambda_i} + \sum_{i=n_k+1}^{2n} \frac{\underset{\sim}{\psi}_{iR} \underset{\sim}{\psi}_{iL}^T}{-\lambda_i} \tag{5.19b}$$

where n_k is the number of kept substructure modes.

The last term in Eq. (5.19b) represents the flexibility provided by the deleted high-frequency modes, and will be referred to as the generalized residual flexibility matrix. This residual flexibility matrix can be written in two ways, i.e.

$$\underset{\approx}{B}{}^{-1}_{res} = \sum_{i=n_k+1}^{2n} \frac{\psi_{iR}\, \psi_{iL}^T}{-\lambda_i} \tag{5.20}$$

or

$$\underset{\approx}{B}{}^{-1}_{res} = \underset{\approx}{B}{}^{-1} - \sum_{i=1}^{n_k} \frac{\psi_{iR}\, \psi_{iL}^T}{-\lambda_i} \tag{5.21}$$

The residual attachment modes can be defined in a manner similar to the standard attachment modes, the only difference being the use of $\underset{\approx}{B}_{res}$ instead of $\underset{\approx}{B}$. Thus,

$$\underset{\approx}{\Phi}_{res} = \underset{\approx}{B}{}^{-1}_{res}\, \underset{\approx}{F} \tag{5.22}$$

where $\underset{\approx}{\Phi}_{res}$ is the matrix of residual attachment modes and $\underset{\approx}{F}$ is the matrix containing the unit interface forces.

As was done with standard attachment modes, the velocity portions of the $\underset{\approx}{\Phi}_{res}$ vectors will be set to zero, a situation which occurs naturally if the damping is symmetric and proportional.

Throughout the preceding discussion of attachment modes it was implicitly assumed that $\underset{\approx}{B}{}^{-1}$ existed, but for an unrestrained substructure this will not be the case. Clearly an alternate method of defining attachment modes is in order for substructures containing

rigid-body degrees of freedom. Two types of attachment modes for unrestrained substructures will be discussed.

When a unit force is applied to an interface degree of freedom of an unrestrained substructure, the substructure will exhibit both rigid-body and elastic motion. If the substructure is assumed to possess some sort of damping of elastic modes, the body will come to a pseudo-equilibrium state where the rigid-body acceleration still exists, but all elastic motion has ceased. Since no relative motion occurs in the substructure when the pseudo-equilibrium state has been reached, the damping terms will produce no internal forces. This argument is the basis for neglecting the damping term when the so-called "inertia-relief attachment modes" are calculated. The inertia-relief attachment modes were first introduced by Rubin (Ref.22), but have been derived by Craig (Ref. 6) in a much cleaner manner.

Since the inertia-relief attachment modes for undamped systems have been presented in numerous articles (Refs. 4, 6, 7, 22) they will not be developed here. Basically, the procedure used to calculate the inertia-relief shape is to subtract the D'Alembert forces from the original unit interface force vector, thereby creating a projection of the interface force vector which does not excite the rigid-body modes. This projected force vector is then applied to the substructure after it has been constrained in an appropriate statically-determinate manner. The deflection shapes that result are the inertia-relief attachment modes. Residual inertia-relief attachment modes can also be developed.

Another method of defining attachment modes for unrestrained substructures would be to simply constrain the substructure at user-defined degrees of freedom. The degrees of freedom are chosen such that rigid-body motion is prevented, allowing an equation similar to Eq. (5.10) to be utilized in defining the attachment modes (Ref. 6). If the degrees of freedom of the substructure are partitioned into three groups, the 'i'-interface set, the 'r'-user-defined rigid-body set, and the 'o'-all other degrees of freedom set, Eq. (5.10) can be written as

$$
\begin{bmatrix} k_{oo} & k_{oi} & k_{or} \\ k_{io} & k_{ii} & k_{ir} \\ k_{ro} & k_{ri} & k_{rr} \end{bmatrix} \begin{bmatrix} \phi_{oi} \\ \phi_{ii} \\ o_{ri} \end{bmatrix} = \begin{bmatrix} 0_{oi} \\ I_{ii} \\ R_{ri} \end{bmatrix} \tag{5.23}
$$

where R_{ri} are the reactive forces applied to the 'r' set to prevent rigid-body motion.

The top two rows of Eq. (5.23) yield

$$
\begin{bmatrix} k_{oo} & k_{oi} \\ k_{io} & k_{ii} \end{bmatrix} \begin{bmatrix} \phi_{oi} \\ \phi_{ii} \end{bmatrix} = \begin{bmatrix} 0_{oi} \\ I_{ii} \end{bmatrix} \tag{5.24a}
$$

or

$$
\underset{\approx a}{K} \underset{\approx a}{\phi} = \underset{\approx a}{F} \tag{5.24b}
$$

By the nature of its development, the $\underset{\approx a}{K}$ matrix used in Eq. (5.24b) is invertible; hence, $\underset{\approx a}{\phi}$ is readily obtained. The attachment modes formed in this manner will be called restrained attachment modes.

The above development is similar to the one used in defining the inertia-relief attachment modes, except that when the projected force vector is applied to the system no reactive forces (R_{ri}) are necessary to prevent rigid-body motion. Of course, no matter which type of attachment mode is used for the unconstrained substructure, it must be augmented by a set of zeros in the velocity positions to become a generalized displacement Ritz vector of length 2n.

As a conclusion to this discussion of attachment modes, it should be noted that the truncated substructure modes are not necessary to the formation of the attachment modes described (i.e. standard, residual, inertia-relief, or restrained attachment modes). Hence, only the substructure modes kept explicitly as Ritz vectors need to be obtained from the substructure eigenproblem. This is in contrast to the attachment modes utilized by Chung (Refs. 2, 3), which are formed directly from the high-frequency modes not used explicitly as Ritz vectors, therefore necessitating the complete solution of the sub-structure eigenproblem.

Chapter 6

COMPUTATIONAL CONSIDERATIONS

In this chapter, several ideas introduced previously will be examined in greater detail. The topics to be considered include the order and type of the system eigenproblem, the issue of including the interface velocity constraints, and, finally, the computation of the state vector attachment modes.

Equation (5.1) can be substituted into the coupled system equation of motion (Eq. (4.28)), resulting in

$$\underset{\approx}{A}_{sys}\; \dot{\underset{\sim}{\eta}}_{sys} \;+\; \underset{\approx}{B}_{sys}\; \underset{\sim}{\eta}_{sys} \;=\; \underset{\sim}{F}_{sys} \tag{6.1}$$

where

$$\underset{\approx}{A}_{sys} \;=\; \underset{\approx}{C}^{T}\; \underset{\approx}{\Phi}^{T}\; \underset{\approx}{A}_{bk}\; \underset{\approx}{\Phi}\; \underset{\approx}{C}$$

$$\underset{\approx}{B}_{sys} \;=\; \underset{\approx}{C}^{T}\; \underset{\approx}{\Phi}^{T}\; \underset{\approx}{B}_{bk}\; \underset{\approx}{\Phi}\; \underset{\approx}{C}$$

and

$$\underset{\approx}{F}_{sys} \;=\; \underset{\approx}{C}^{T}\; \underset{\approx}{\Phi}^{T}\; \underset{\sim}{F}$$

Notice that in this form of the equation of motion, no distinction is made between the standard and the adjoint Ritz vectors, since they are taken to be identical.

The system eigenproblem can be developed from Eq. (6.1) using the substitution $\underset{\sim}{\eta}_{sys} = \underset{\sim}{\psi}_{sys} e^{\omega t}$, i.e.

$$\omega \; \underset{\approx}{A}_{sys} \; \underset{\sim}{\psi}_{sys} \; + \; \underset{\approx}{B}_{sys} \; \underset{\sim}{\psi}_{sys} \; = \; \underset{\sim}{0} \qquad (6.2)$$

Two points, both important to the solution of the above system eigen-problem, will now be discussed.

First, it should be clear that the $\underset{\approx}{A}_{sys}$ and $\underset{\approx}{B}_{sys}$ matrices are complex since the component modes which are used in the formation of the system matrices are complex in nature. This fact will of course make it necessary that a complex eigensolver be available.

A second very critical point to be considered when studying the system eigenproblem is the dimensions of the system matrices involved. From Eqs. (4.24) and (6.1) it is clear that the order of $\underset{\approx}{A}_{sys}$ and $\underset{\approx}{B}_{sys}$ is

$$N_{sys} \; = \; N_{\alpha} + N_{\beta} - N_c \qquad (6.3)$$

where N_{α} and N_{β} are the total number of Ritz vectors used to describe substructures α and β respectively, and N_c is the number of interface constraints imposed upon the system.

As mentioned in the section on constraints, N_c can be equated with N_i , $2N_i$, or N_{av} where N_i is the number of physical interface degrees of freedom and N_{av} is the number of constraint equations utilized when the geometric compatibility conditions are satisfied in some average sense. Of course, $N_c = N_i$ implies that only interface displacement compatibility is satisfied, and when $N_c = 2N_i$ both interface displacement and velocity compatibilities are enforced. If the geometric interface compatibility is enforced in an average sense, Eqs. (4.7) through (4.10) dictate that the interface

force compatibility must also be satisfied in an approximate fashion, a situation not considered in this thesis.

The size of N_{sys} is certainly a factor when considering whether or not to enforce the velocity constraints. If N_{sys} is desired to be as small as possible without altering N_α or N_β, it is clear that the velocity constraints should be enforced. Of course, if a larger system eigenproblem can be tolerated, the effort of enforcing the velocity constraints can be avoided by enforcing only the displacement compatibility.

A computational point in favor of constraining the interface velocity coordinates is the conditioning of the $\underset{\approx sys}{A}$ matrix that occurs when the velocity constraints are included in the formulation. This conditioning will be demonstrated on an axial rod with two substructures, i.e.
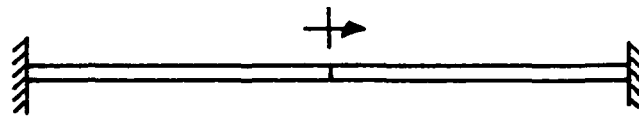
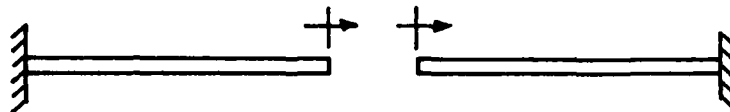Figure 6.1(a). One degree of freedom axial rod.

Figure 6.2(b). One degree of freedom substructures α and β.

The state vector form of the equations of motion will be used to describe the substructures, even though the substructures will be

assumed to be undamped. The state vector equation of motion for the single element substructures can be written as

$$
\begin{bmatrix} 0 & 1 \\ 1 & 0 \end{bmatrix} \begin{Bmatrix} \ddot{v} \\ \dot{x} \end{Bmatrix} + \begin{bmatrix} -1 & 0 \\ 0 & 1 \end{bmatrix} \begin{Bmatrix} v \\ x \end{Bmatrix} = \begin{Bmatrix} 0 \\ 0 \end{Bmatrix} \tag{6.4}
$$

The substructure equations of motion will be coupled twice, first with interface displacement and velocity coordinate constraints, and second with displacement constraints only.

It may be shown that the coupled system equation of motion for the case of both displacement and velocity constraints is

$$
\begin{bmatrix} 0 & 2 \\ 2 & 0 \end{bmatrix} \begin{Bmatrix} \dot{v}_\alpha \\ \dot{x}_\alpha \end{Bmatrix} + \begin{bmatrix} -2 & 0 \\ 0 & 2 \end{bmatrix} \begin{Bmatrix} v_\alpha \\ x_\alpha \end{Bmatrix} = \begin{Bmatrix} 0 \\ 0 \end{Bmatrix} \tag{6.5}
$$

The characteristic equation for the above system equation of motion is

$$
\omega^2 + 1 = 0 \tag{6.6}
$$

When only the displacement constraints are enforced, the coupled system equation of motion is

$$
\begin{bmatrix} 0 & 1 & 0 \\ 1 & 0 & 1 \\ 0 & 1 & 0 \end{bmatrix} \begin{Bmatrix} \dot{v}_\alpha \\ \dot{x}_\alpha \\ \dot{v}_\beta \end{Bmatrix} + \begin{bmatrix} -1 & 0 & 0 \\ 0 & 2 & 0 \\ 0 & 0 & -1 \end{bmatrix} \begin{Bmatrix} v_\alpha \\ x_\alpha \\ v_\beta \end{Bmatrix} = \begin{Bmatrix} 0 \\ 0 \\ 0 \end{Bmatrix} \tag{6.7}
$$

The characteristic equation for this equation of motion is

$$
\omega^2 + 1 = 0 \tag{6.8}
$$

Clearly the same solution is obtained whether or not the velocity constraints are enforced. However, there are two reasons why the eigenproblem developed from Eq. (6.5) might be easier to solve than the eigenproblem resulting from Eq. (6.7). First, Eq. (6.5) has fewer degrees of freedom than Eq. (6.7), and second, the $\underset{\approx}{A}_{sys}$ matrix in Eq. (6.5) is invertible, whereas $\underset{\approx}{A}_{sys}$ in Eq. (6.7) is singular. As mentioned previously, if the $\underset{\approx}{A}$ matrix is noninvertible the generalized eigenproblem cannot be transformed into a standard eigenproblem, so in this case a standard eigensolver would be of no use in the solution of the system eigenproblem.

As a conclusion to this chapter, the subject of attachment modes will be examined from a computational point of view. Of the four types of attachment modes developed in Chapter 5, all but the generalized residual attachment modes will be a set of unconditionally real vectors. For general damping, the generalized residual flexibility modes will be complex; however, for the special case of symmetric proportional damping, it can be shown that the generalized residual attachment modes are real.

It has been previously noted that the adjoint eigenvectors are not used as Ritz vectors, thus apparently eliminating the need for the solution to the adjoint eigenproblem. Clearly, this is not the case if generalized residual attachment modes are employed as substructure Ritz vectors. As can be seen in Eqs. (5.21) and (5.22), the left-hand eigenvectors are necessary to the formation of the generalized flexibility matrix, and are therefore required to form the generalized residual attachment modes.

An alternative to the generalized residual attachment modes for restrained substructures are the standard attachment modes defined in Eq. (5.10). The solution of a set of linear algebraic equations is all that is required in the formation of this type of attachment mode.

For unrestrained substructures, two types of attachment modes have been derived, namely the generalized inertia-relief attachment modes and the restrained attachment modes. The calculation of the inertia-relief attachment modes involves manipulation of the substructure mass matrix followed by a solution of a set of algebraic equations (Ref. 6). As was required in the formation of the standard attachment modes, the calculation of the restrained attachment modes requires only the solution to a set of linear algebraic equations involving the substructure stiffness matrix (see Eq. (5.23)).

It will be shown in the following chapter that the system accuracy obtained when using the rather unsophisticated standard or restrained attachment modes is comparable to the accuracy exhibited when generalized residual or inertia-relief attachment modes are used. This fact, coupled with the relative ease of computing standard and restrained attachment modes, forms the basis of a computational preference for the standard attachment modes when dealing with constrained substructures, and for restrained attachment modes when dealing with unconstrained substructures.

Chapter 7

EXAMPLE PROBLEMS

The results of several test problems are presented in this chapter. For each problem the approximate system eigenvalues are compared with those of the exact system.

EXAMPLE 1.

The first example presented is a clamped-clamped beam with 18 physical degrees of freedom. The beam is substructured as follows:

$$A = E = L = \rho = 1$$

Clamped-Clamped System
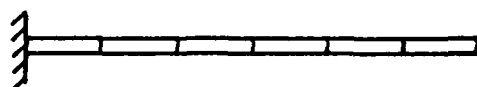
Substructure α

Substructure β

Figure 7.1 - 18 DOF Clamped-Clamped Beam

The two cantilevered substructures have identical mass and stiffness properties, but the damping associated with each substructure is different. At the substructure level, the damping matrix is taken to be proportional to the stiffness matrix, as defined in the following equations:

$$[C]_\alpha = \frac{1}{48} [K]_\alpha$$

and

$$[C]_\beta = \frac{1}{96} [K]_\beta$$

Of course, when the system is coupled, the system damping matrix is not proportional to the system stiffness matrix.

Since the exact beam is represented by 18 physical degrees of freedom, the exact system eigenproblem will have 36 degrees of freedom due to the state vector representation of the equation of motion. The Ritz vectors which were used to represent the substructures are accounted for below.

Substructure α :   6   pairs of complex conjugate modes
                             2   real residual attachment modes

                             14   total

Substructure β :   4   pairs of complex conjugate modes
                             2   real residual attachment modes

                             10   total

Both displacement and velocity compatibility at the interface were enforced; therefore, the approximate system has a total of 20 degrees

of freedom. Table 7.1.1 presents a comparison of the system eigenvalues, where the complex eigenvalues are written as

$$\omega = \sigma + i\omega_d$$

where $-\sigma$ is the modal damping coefficient and

ω_d is the damped natural frequency

Also included for this example is a comparison case in which the same number of eigenmodes for each substructure were employed, but no attachment modes were included as Ritz vectors. The results for this second case are presented in Table 7.1.2.

A comparison of Tables 7.1.1 and 7.1.2 clearly shows the rather impressive increase in accuracy provided by the inclusion of attachment modes as Ritz vectors. This parallels the results found by Chung (Ref. 2). When the attachment modes were included, the first 5 pairs of system eigenvalues exhibit excellent accuracy, with less than a 2% maximum error in the damping coefficient, and less than a 1% maximum error in the damped natural frequency.

Eigenvalue Number	Exact		Approximate		σ % Error	ω_d % Error
	σ	ω_d	σ	ω_d		
1	-.426E-3	.224E0	-.426E-3	.224E0	.019	.009
2	-.304E-2	.617E0	-.304E-2	.617E0	.029	.045
3	-.125E-1	.121E+1	-.126E-1	.121E+1	.413	.077
4	-.332E-1	.200E+1	-.338E-1	.202E+1	1.753	.952
5	-.747E-1	.300E+1	-.743E-1	.300E+1	-.592	.082
6	-.150E0	.421E+1	-.167E0	.434E+1	11.560	3.033
7	-.263E0	.565E+1	-.251E0	.585E+1	-4.425	3.634
8	-.447E0	.730E+1	-.528E0	.747E+1	18.040	2.254

TABLE 7.1.1 Comparison of Exact and Approximate System Eigenvalues for Example 1, Attachment Modes Included. All eigenvalues listed are one of a pair of complex conjugate system eigenvalues.

Eigenvalue Number	Exact		Approximate		σ	ω_d
	σ	ω_d	σ	ω_d	% Error	% Error
1	-.426E-3	.224E0	-.486E-3	.235E0	14.139	5.013
2	-.304E-2	.617E0	-.311E-2	.646E0	2.590	4.742
3	-.125E-1	.121E+1	-.139E-1	.124E0	11.494	2.315
4	-.332E-1	.200E+1	-.410E-1	.224E+1	23.417	11.842
5	-.747E-1	.300E+1	-.723E-1	.303E+1	-3.211	0.970
6	-.150E0	.421E+1	-.209E0	.463E+1	39.779	9.981
7	-.263E0	.565E+1	-.237E0	.619E+1	-9.741	9.696
8	-.447E0	.730E+1	-.580E0	.762E+1	29.712	4.341

TABLE 7.1.2   Comparison of Exact and Approximate System Eigenvalues for Example 1, No Attachment Modes. All eigenvalues listed are one of a pair of complex conjugate system eigenvalues.

EXAMPLE 2.

The second example is a free-free beam with the following geometry and substructuring:

$$A = E = L = \rho = 1$$

Free-Free System
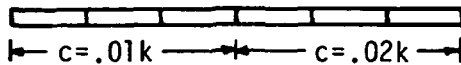
Substructure α
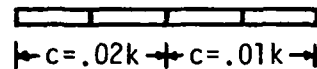
Substructure β

Figure 7.2 - 22 DOF Free-Free Beam

The mass and stiffness properties of the two free-free components are identical, but each has its own damping characteristics. As can be seen in Figure 7.2, the damping is not proportional at the substructure level; hence, the system is obviously not proportionally damped.

Two types of attachment modes were applied to this problem, and the breakdown of the Ritz vectors for each case is given below.

Case 1.   Substructure α :   6   pairs of flexible modes
                                  4   rigid-body modes
                                  2   generalized inertia-relief
                                  __   attachment modes

                                 18   total

           Substructure β :   4   pairs of flexible modes
                                  4   rigid-body modes
                                  2   generalized inertia-relief
                                  __   attachment modes

                                 14   total

Case 2.   Substructure α :   6   pairs of flexible modes
                                  4   rigid-body modes
                                  2   restrained substructure
                                  __   attachment modes

                                 18   total

           Substructure β :   4   pairs of flexible modes
                                  4   rigid-body modes
                                  2   restrained substructure
                                  __   attachment modes

                                 14   total

    The results of Case 1 are presented in Table 7.2.1 and those of
Case 2 in Table 7.2.2. Displacement and velocity compatibility were
both enforced at the interface, resulting in an eigenproblem of order
28 for both cases. The exact eigenproblem is of order 44.

    The primary goal of this example is to establish the validity
of the definition of the rigid-body modes when a state vector approach
is used. Also of interest is the comparison between the accuracies of
the coupled system when inertia-relief attachment modes are used versus
the use of restrained substructure attachment modes.

Although the eigenvalues corresponding to the system rigid-body modes were suppressed from Tables 7.2.1 and 7.2.2, the system eigensolution did indeed contain 4 rigid-body modes, as would be expected from the state vector model of the structure. This fact, along with the accuracy displayed by the flexible modes, appears to justify the definition of the state vector rigid-body modes given in Eq. (5.9).

When Tables 7.2.1 and 7.2.2 are compared, it is seen that both cases produce 8 complex conjugate pairs of system eigenvalues with a maximum error of approximately 5%. It should also be noted that the rather simple restrained attachment modes (7.2.2) produce slightly more accurate eigenvalues for this system than do the generalized inertia-relief attachment modes (Table 7.2.1).

Eigenvalue Number	Exact		Approximate		σ % Error	ω_d % Error
	σ	ω_d	σ	ω_d		
1	-.473E-3	.224E0	-.490E-3	.224E0	3.692	-.001
2	-.312E-2	.617E0	-.318E-2	.617E0	2.145	.015
3	-.109E-1	.121E+1	-.110E-1	.121E+1	.993	.027
4	-.300E-1	.200E+1	-.314E-1	.201E+1	4.712	.338
5	-.671E-1	.300E+1	-.673E-1	.300E+1	.267	.021
6	-.131E0	.421E+1	-.138E0	.426E+1	5.307	1.226
7	-.240E0	.563E+1	-.251E0	.570E+1	4.464	1.248
8	-.395E0	.727E+1	-.407E0	.735E+1	2.885	1.102
9	-.621E0	.902E+1	-.749E0	.972E+1	20.637	7.674
10	-.109E+1	.120E+2	-.112E+1	.121E+2	2.233	.928

Note: Only eigenvalues corresponding to flexible modes are included in table.

TABLE 7.2.1   Comparison of Exact and Approximate System Eigenvalues for Example 2, Case 1. (Generalized inertia-relief attachment modes). All eigenvalues are one of a pair of complex conjugate system eigenvalues.

62

Eigenvalue Number	Exact		Approximate		σ % Error	ω_d % Error
	σ	ω_d	σ	ω_d		
1	-.473E-3	.224E0	-.474E-3	.224E0	.251	.006
2	-.312E-2	.617E0	-.312E-2	.617E0	.176	.021
3	-.109E-1	.121E+1	-.109E-1	.121E+1	.186	.039
4	-.300E-1	.200E+1	-.302E-1	.201E+1	.943	.345
5	-.671E-1	.300E+1	-.673E-1	.300E+1	.211	.052
6	-.131E0	.421E+1	-.135E0	.426E+1	2.660	1.241
7	-.240E0	.563E+1	-.247E0	.570E+1	3.005	1.283
8	-.395E0	.727E+1	-.405E0	.735E+1	2.415	1.150
9	-.621E0	.902E+1	-.732E0	.972E+1	17.865	7.692
10	-.109E+1	.120E+2	-.112E+1	.121E+2	2.266	1.038

Note: Only eigenvalues corresponding to flexible modes are included in table.

TABLE 7.2.2 Comparison of Exact and Approximate System Eigenvalues for Example 2, Case 2. (Restrained substructure attachment modes). All eigenvalues are one of a pair of complex conjugate system eigenvalues.
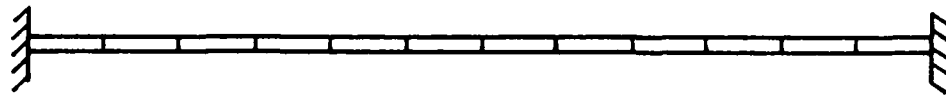
EXAMPLE 3.

The third example presented is a clamped-clamped beam with the geometry and substructuring shown below.

$$E = A = L = \rho = 1$$

Clamped-Clamped System
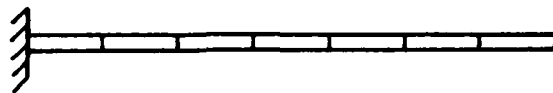
Substructure α

Substructure β

Figure 7.3 - 22 DOF Clamped-Clamped Beam

In the previous examples the damping matrix was non-proportional at the system level, but was always symmetric in form. The element damping matrices used in this problem are skew-symmetric in form, and are defined in the following equations:

$$[C]_\alpha^e = \frac{1}{20} [C]^e$$

$$[C]_\beta^e = \frac{1}{40} [C]^e$$

where

$$[c]^e = \begin{bmatrix} 5 & 1 & 1 & 1 \\ -1 & 5 & 1 & 1 \\ -1 & -1 & 5 & 1 \\ -1 & -1 & -1 & 5 \end{bmatrix}$$

The Ritz vectors utilized in the coupling procedure are now described.

Substructure α :   13   complex modes
                    2   real standard attachment
                             modes
                    —
                    15   total

Substructure β :   10   complex modes
                      2   real standard attachment
                             modes
                    —
                    12   total

The effect of not enforcing velocity compatibility at the interface is examined in this example. Case 1 considers the situation when both displacement and velocity constraints are enforced, and Case 2 concerns itself with displacement compatibility only. Comparisons between the exact and the approximate system eigenvalues for the two cases are presented in Tables 7.3.1 and 7.3.2 respectively.

An interesting feature of this example, which poses no problem for the coupling procedure, is the fact that not all of the modes appear in complex conjugate pairs as in Examples 1 and 2. As can be

seen in either Table. 7.3.1 or 7.3.2, the first two eigenvalues have no oscillatory part (ω_d).

If the two tables are compared, it can be seen that both cases yield excellent accuracy in the low-frequency range. It should also be noted that, for this system, the case in which the velocity constraints are not enforced actually produces slightly more accurate eigenvalues than the case containing enforced velocity constraints. Hence, the fact that velocity constraints do not necessarily need to be enforced appears to be verified.

Eigenvalue Number	Exact		Approximate		σ % Error	ω_d % Error
	σ	ω_d	σ	ω_d		
1*	-.607E-1	0	-.607E-1	.245E-13	-.001	.000
2*	-.399E0	0	-.399E0	-.159E-13	-.003	.000
3	-.254E0	.343E0	-.254E0	.343E0	.025	.015
4	-.337E0	.770E0	-.337E0	.770E0	.026	-.008
5	-.441E0	.133E+1	-.443E0	.133E+1	.356	.182
6	-.574E0	.203E+1	-.573E0	.203E+1	-.222	.048
7	-.738E0	.288E+1	-.751E0	.290E+1	1.842	.455
8	-.922E0	.390E+1	-.910E0	.394E+1	-1.370	.982
9	-.114E+1	.516E+1	-.117E+1	.516E+1	2.650	.073
10	-.122E+1	.656E+1	-.109E+1	.684E+1	-10.568	4.232
11	-.113E+1	.832E+1	-.102E+1	.881E+1	-9.868	5.926

* - This eigenvalue is not a member of a complex conjugate pair; all others are.

TABLE 7.3.1   Comparison of Exact and Approximate System Eigenvalues for Example 3, Case 1.

Eigenvalue Number	Exact		Approximate		σ % Error	ω_d % Error
	σ	ω_d	σ	ω_d		
1*	-.607E-1	0	-.607E-1	.381E-14	-.000	.000
2*	-.399E0	0	-.399E0	-.308E-13	-.000	.000
3	-.254E0	.343E0	-.254E0	.343E0	.003	.002
4	-.337E0	.770E0	-.337E0	.770E0	.001	-.002
5	-.441E0	.133E+1	-.441E0	.133E+1	.043	.027
6	-.574E0	.203E+1	-.574E0	.203E+1	-.029	-.006
7	-.738E0	.288E+1	-.740E0	.289E+1	.234	.093
8	-.922E0	.390E+1	-.920E0	.390E+1	-.250	.054
9	-.114E+1	.516E+1	-.115E+1	.517E+1	.541	.294
10	-.122E+1	.656E+1	-.119E+1	.660E+1	-2.637	.590
11	-.113E+1	.832E+1	-.923E0	.875E+1	-18.541	5.189

* - This eigenvalue is <u>not</u> a member of a complex conjugate pair; all others are.

TABLE 7.3.2   Comparison of Exact and Approximate System Eigenvalues for Example 3, Case 2.

EXAMPLE 4.

In this final example to be presented, a pin-jointed planar truss structure will be considered. The geometry and substructuring of the system are as follows:

A = E = L = ρ = 1

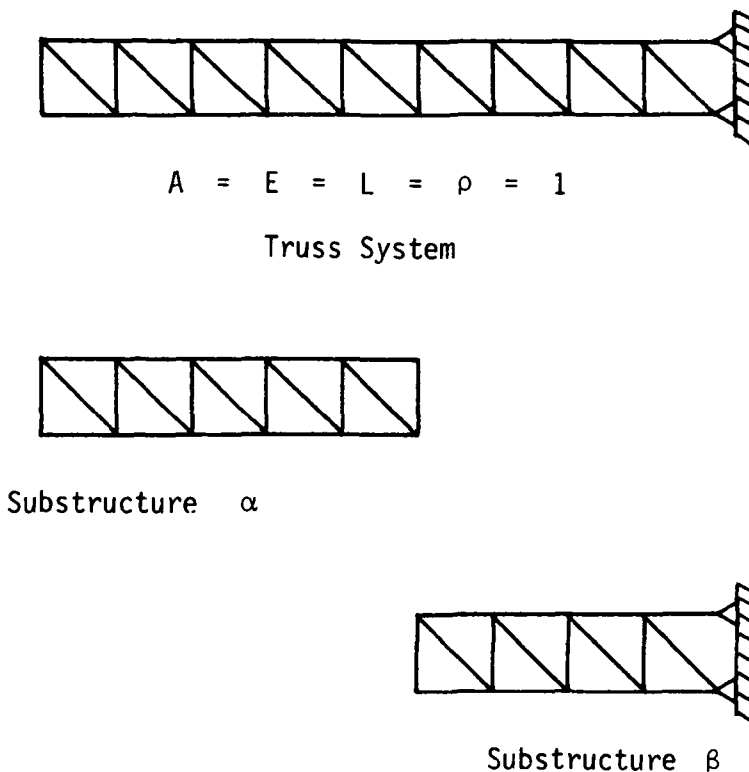Truss System

Substructure α

Substructure β

Figure 7.4 - 36 DOF Pin-Jointed Truss.

For the purpose of this example, only the upper and lower horizontal members are considered damped. The form of the element damping matrix for each substructure is given by the following equations:

$$[C]^e_\alpha = .05 \, [C]^e$$

$$[C]^e_\beta = .075 \, [C]^e$$

where

$$[C]^e = \begin{bmatrix} 1 & 1 \\ -1 & 1 \end{bmatrix}$$

The nature of this problem allows us to examine the ability of the coupling procedure to deal with potential problems such as non-symmetric damping and rigid-body modes simultaneously. The substructure Ritz vectors are given below.

Substructure α :	18	complex flexible modes
	6	real rigid-body modes
	4	real restrained substructure attachment modes
	__	
	28	total

Substructure β :	14	complex flexible modes
	4	real standard attachment modes
	__	
	18	total

Both displacement and velocity coordinates are constrained at the interface; therefore, the approximate system eigenproblem is of order 38. The exact system eigenproblem is of order 72. A comparison between the exact and the approximate eigenvalues is given in Table 7.4.

As Table 7.4 indicates, the coupling procedure provides 8 pairs of complex conjugate system eigenvalues that have a maximum error of less than 4% in the damping coefficient. The damped natural frequencies are commonly two orders of magnitude larger than the damping coefficients, and as Table 7.4 shows, the damped natural frequencies are usually more accurate than the damping coefficients. The ability of the coupling procedure to approximate this system containing both nonsymmetric state matrices and rigid-body modes (at the substructure level) reinforces the belief that the method can be applied effectively to much larger complex structural systems.

Eigenvalue Number	Exact		Approximate		σ	ω_d
	σ	ω_d	σ	ω_d	% Error	% Error
1	-.852E-3	.209E0	-.825E-3	.210E0	-3.266	.524
2	-.874E-2	.195E0	-.883E-2	.196E0	.993	.580
3	-.695E-3	.151E0	-.678E-3	.152E0	-2.480	.634
4	-.622E-3	.951E-1	-.621E-3	.952E-1	-.239	.034
5	-.726E-2	.646E-1	-.729E-2	.651E-1	.430	.743
6	-.499E-3	.421E-1	-.498E-3	.422E-1	-.197	.105
7	-.112E-3	.853E-2	-.112E-3	.853E-2	.026	.004
8	-.127E-2	.262E0	-.128E-2	.265E0	.939	1.275
9	-.556E-2	.304E0	-.650E-2	.308E0	16.861	1.338
10	-.234E-2	.320E0	-.156E-2	.327E0	-33.258	2.293
11	-.934E-2	.323E0	-.935E-2	.329E0	.128	2.080
12	-.108E-2	.365E0	-.111E-2	.369E0	2.728	.993
13	-.735E-2	.381E0	-.845E-2	.395E0	14.921	3.638

TABLE 7.4   Comparison of Exact and Approximate System Eigenvalues for Example 4. All eigenvalues shown are one of a pair of complex conjugates.

Chapter 8

CONCLUSIONS AND RECOMMENDATIONS

Presented in this thesis is a procedure for the coupling of generally damped substructures for dynamic analysis. No assumptions of proportionality or even symmetry of the defining matrices (M, C, or K) are necessary. The method is developed from a variational principle which essentially results in a state vector representation of the system. Since low-frequency substructure modes along with a set of generalized attachment modes are employed as substructure Ritz vectors, the coupling procedure can be described as a "generalized component mode synthesis technique."

The numerical test problems indicate that the coupling procedure produces accurate system eigenvalues in the low-frequency range. Typically, the damped natural frequencies (ω_d) are more accurate than the modal damping coefficients (σ). It has also been shown numerically that it is not mandatory to enforce velocity compatibility between substructures, but that its enforcement can sometimes be advantageous. The rather unsophisticated attachment modes utilized appear to represent the truncated high-frequency modes quite well, thereby making the complete solution of the substructure eigenproblem unnecessary.

On the basis of the example problems, it appears that the number of coupled system eigenvalues which exhibit extreme accuracy is at least as large as the minimum number of flexible modes used as Ritz vectors for either substructure. If this could be substantiated analytically, or even empirically, it would be a great aid to the

analyst, since an a priori estimate of system accuracy might dictate the number of substructure modes to be retained in the analysis.

Since a knowledge of the system modes is often of great importance, the effect of substructuring on the accuracy of the system modes needs to be quantitatively explored. This suggests the establishment of a suitable error norm which would quantify the error existing between the approximate and exact system eigenvectors as a topic for future consideration.

Finally, any technique that efficiently produces substructure Ritz vectors which lead to acceptable system accuracy should be explored in detail. Hale's "subspace iteration" (Ref. 11) and Wilson's iterative procedure (Ref. 25) should both be examined further in order to determine their computational merits as producers of substructure Ritz vectors.

Appendix

Briefly presented in this appendix are some of the mathematical tools used throughout the development of the coupling procedure. The principal topics discussed will be adjoint differential equations, adjoint eigenproblems, and variational principles for non-self-adjoint systems.

1. Adjoint Differential Equations

The introduction of operator notation will prove very convenient in our discussion of adjoint differential equations, and is now demonstrated in the following example:

$$\underset{\approx}{M}\ddot{\underset{\sim}{x}} + \underset{\approx}{C}\dot{\underset{\sim}{x}} + \underset{\approx}{K}\underset{\sim}{x} = \underset{\sim}{F} \qquad (A.1)$$

or

$$\underset{\approx}{L}(\underset{\sim}{x}) = \underset{\sim}{F} \qquad (A.2)$$

where

$$\underset{\approx}{L}(\ ) = \underset{\approx}{M}(\ddot{\ }) + \underset{\approx}{C}(\dot{\ }) + \underset{\approx}{K}(\ ) \qquad (A.3)$$

In the above equations, $\underset{\approx}{L}$ is the differential operator corresponding to Eq. (A.1). The adjoint differential operator, $\underset{\approx}{L}^*$, is related to $\underset{\approx}{L}$ in the following way:

$$<\underset{\approx}{L}(\underset{\sim}{x}),\underset{\sim}{y}> = <\underset{\sim}{x},\underset{\approx}{L}^*(\underset{\sim}{y})> \qquad (A.4)$$

where < > denotes an inner product.

It should be clear that the form of the adjoint operator is intimately associated with the choice of the inner product used in Eq.

74

(A.4). The inner product usually adopted when working with differential equations is

$$<\underset{\sim}{x},\underset{\sim}{y}> = \int_0^t \underset{\sim}{y}^T \underset{\approx}{L}(\underset{\sim}{x}) \, dt \qquad (A.5)$$

Using the above inner product, we can now find $\underset{\approx}{L}^*$ corresponding to the example $\underset{\approx}{L}$ defined in Eq. (A.3). This is done as follows:

$$<\underset{\approx}{L}(\underset{\sim}{x}), \underset{\sim}{y}> = \int_0^t \underset{\sim}{y}^T \underset{\approx}{L}(\underset{\sim}{x}) \, dt$$

$$= \int_0^t (\underset{\sim}{y}^T \underset{\approx}{M}\underset{\sim}{\ddot{x}} + \underset{\sim}{y}^T \underset{\approx}{C}\underset{\sim}{\dot{x}} + \underset{\sim}{y}^T \underset{\approx}{K}\underset{\sim}{x}) \, dt$$

$$= [\underset{\sim}{y}^T \underset{\approx}{M}\underset{\sim}{\dot{x}} - \underset{\sim}{\dot{y}}^T \underset{\approx}{M}\underset{\sim}{x} + \underset{\sim}{y}^T \underset{\approx}{C}\underset{\sim}{x}]_0^t \qquad (A.6)$$

$$+ \int_0^t (\underset{\sim}{\ddot{y}}^T \underset{\approx}{M}\underset{\sim}{x} - \underset{\sim}{\dot{y}}^T \underset{\approx}{C}\underset{\sim}{x} + \underset{\sim}{y}^T \underset{\approx}{K}\underset{\sim}{x}) \, dt$$

$$= [\text{boundary terms}]_0^t$$

$$+ \int_0^t \underset{\sim}{x}^T (\underset{\approx}{M}^T\underset{\sim}{\ddot{y}} - \underset{\approx}{C}^T\underset{\sim}{\dot{y}} + \underset{\approx}{K}^T\underset{\sim}{y}) \, dt$$

Since variations on the time boundary are disallowed for this system, only the integral portion of the right-hand side of Eq. (A.6) is non-vanishing. This fact implies that $\underset{\approx}{L}^*$ will be a "formal adjoint

operator," i.e. an adjoint operator with no consideration of boundary terms. A comparison of Eqs. (A.4) and (A.6) easily shows that

$$\underset{\approx}{L}*(\ ) = \underset{\approx}{M}^T(\ddot{\ }) - \underset{\approx}{C}^T(\dot{\ }) + \underset{\approx}{K}^T(\ ) \qquad (A.7)$$

Thus, the differential equation corresponding to $\underset{\approx}{L}*$ is

$$\underset{\approx}{M}^T\underset{\sim}{\ddot{y}} - \underset{\approx}{C}^T\underset{\sim}{\dot{y}} + \underset{\approx}{K}^T\underset{\sim}{y} = \underset{\sim}{F}* \qquad (A.8)$$

where $\underset{\sim}{F}*$ represents the somewhat abstract "adjoint force" vector. Fortunately, a determination of $\underset{\sim}{F}*$ is not necessary for the purposes of this thesis, and is included in Eq. (A.8) only to provide symmetry with Eq. (A.1).

Logically, if the differential operator and its adjoint are identical $(\underset{\approx}{L} = \underset{\approx}{L}*)$, the differential equation will be termed self-adjoint. When Eqs. (A.1) and (A.8) are compared, it is not difficult to extrapolate to the fact that differential equations possessing odd-order derivatives will always be non-self-adjoint.

The adjoint differential equation leads, naturally, to the adjoint eigenproblem, which will now be considered.

2.   The Adjoint Eigenproblem.

Consider the following first-order linear differential equation:

$$\underset{\approx\sim}{A}\underset{\sim}{\dot{X}} + \underset{\approx\sim}{B}\underset{\sim}{X} = \underset{\sim}{0} \qquad (A.9)$$

and its adjoint

$$-\underset{\approx}{A}^T\underset{\sim}{\dot{Y}} + \underset{\approx}{B}^T\underset{\sim}{Y} = \underset{\sim}{0} \qquad (A.10)$$

The usual eigenproblem can be formed from Eq. (A.9) with the substitution

$$\underset{\sim}{X} = \underset{\sim}{\psi}_R e^{\lambda t} \tag{A.11}$$

and the adjoint eigenproblem is similarly formed from Eq. (A.10) with

$$\underset{\sim}{Y} = \underset{\sim}{\psi}_L e^{-\lambda t} \tag{A.12}$$

It should be noted that the exponent in Eq. (A.12) contains a minus sign, whereas the exponent in Eq. (A.11) does not.

The usual eigenproblem takes the form

$$\lambda \underset{\approx}{A} \underset{\sim}{\psi}_R + \underset{\approx}{B} \underset{\sim}{\psi}_R = \underset{\sim}{0} \tag{A.13}$$

and the adjoint eigenproblem is seen to be

$$\lambda \underset{\approx}{A}^T \underset{\sim}{\psi}_L + \underset{\approx}{B}^T \underset{\sim}{\psi}_L = \underset{\sim}{0} \tag{A.14}$$

The adjoint eigenproblem is sometimes referred to as the "left-hand" eigenproblem. The reason for this terminology is obvious when the transpose of Eq. (A.14) is considered, i.e.

$$\lambda \underset{\sim}{\psi}_L^T \underset{\approx}{A} + \underset{\sim}{\psi}_L^T \underset{\approx}{B} = \underset{\sim}{0} \tag{A.15}$$

The eigenvectors in the above equation are on the left side of the $\underset{\approx}{A}$ and $\underset{\approx}{B}$ matrices, whereas in Eq. (A.13) the eigenvectors are on the right side. Several important properties of the left and right-hand eigenproblems will now be developed.

Property 1. The left and right eigenvalues are identical.

Proof: Writing the characteristic determinant of Eqs. (A.13) and (A.14) we have

$$DET \; |\; \lambda \underset{\approx}{A} + \underset{\approx}{B} \;| \; = \; 0 \qquad (A.16)$$

and

$$DET \; |\; \lambda \underset{\approx}{A}^T + \underset{\approx}{B}^T \;|$$
$$= \; DET \; |\; (\lambda \underset{\approx}{A} + \underset{\approx}{B})^T \;| \; = \; 0 \qquad (A.17)$$

Since the determinant of a matrix and its transpose are equal, the determinants in Eqs. (A.16) and (A.17) will yield identical characteristic equations, and therefore identical eigenvalues.

Property 2. Bi-orthogonality, i.e.

$$\underset{\sim}{\psi}_{L_i}^T \; \underset{\approx}{A} \underset{\sim}{\psi}_{R_j} \; = \; 0 \qquad (A.18)$$

$$i \neq j$$

$$\underset{\sim}{\psi}_{L_i}^T \; \underset{\approx}{B} \underset{\sim}{\psi}_{R_j} \; = \; 0 \qquad (A.19)$$

Proof: If Eq. (A.13) is written for the ith eigenpair, and Eq. (A.15) for the jth eigenpair, we have

$$\lambda_i \underset{\approx}{A} \underset{\sim}{\psi}_{Ri} + \underset{\approx}{B} \underset{\sim}{\psi}_{Ri} \; = \; \underset{\sim}{0} \qquad (A.20)$$

and

$$\lambda_j \underset{\sim}{\psi}_{Lj}^T \underset{\approx}{A} + \underset{\sim}{\psi}_{Lj}^T \underset{\approx}{B} \; = \; \underset{\sim}{0} \qquad (A.21)$$

Premultiplying Eq. (A.20) by ψ_{Lj}^T and postmultiplying Eq. (A.21) by ψ_{Ri} results in

$$\lambda_i \psi_{Lj}^T A \psi_{Ri} + \psi_{Lj}^T B \psi_{Ri} = 0 \qquad \text{(A.22)}$$

$$\lambda_j \psi_{Lj}^T A \psi_{Ri} + \psi_{Lj}^T B \psi_{Ri} = 0 \qquad \text{(A.23)}$$

If Eqs. (A.22) and (A.23) are subtracted, the following equation results:

$$(\lambda_i - \lambda_j) \, \psi_{Lj}^T \, A \, \psi_{Ri} = 0 \qquad \text{(A.24)}$$

Assuming distinct eigenvalues $(\lambda_i \neq \lambda_j)$, then Eqs. (A.24) and (A.23) provide the bi-orthogonality conditions,

$$\psi_{Li}^T \, A \, \psi_{Rj} = 0 \qquad \text{(A.25)}$$

and

$$\psi_{Li}^T \, B \, \psi_{Rj} = 0 \qquad \text{(A.26)}$$

Property 3. Bi-orthonormality, i.e.

$$\text{If} \qquad \psi_{Li}^T \, A \, \psi_{Ri} = 1 \ , \qquad \text{(A.27)}$$

$$\text{then} \qquad \psi_{Li}^T \, B \, \psi_{Ri} = -\lambda_i \qquad \text{(A.28)}$$

Proof: Premultiplying Eq. (A.20) by ψ_{Li}^T results in

$$\lambda_i \, \psi_{Li}^T \, A \, \psi_{Ri} + \psi_{Li}^T \, B \, \psi_{Ri} = 0 \qquad \text{(A.29)}$$

If $\psi_{Li}^T \; A \; \psi_{Ri}$ is normalized to unity, then clearly $\psi_{Li}^T \; A \; \psi_{Ri}$ must be equal to $-\lambda_i$.

A very useful property of the adjoint eigenvectors is their ability to uncouple a system of differential equations. For example, assume we have a system of n coupled differential equations such as

$$A\dot{X} + BX = F \tag{A.30}$$

Now, the eigenvector expansion of X can be written as

$$X = \Psi_R \, \eta(t) \tag{A.31}$$

Upon substitution of Eq. (A.31) into Eq. (A.30), the result can be pre-multiplied by Ψ_L^T to produce

$$\Psi_L^T \; A \; \Psi_R \; \dot{\eta}(t) + \Psi_L^T \; B \; \Psi_R \; \eta(t) = \Psi_L^T F \tag{A.32}$$

If the bi-orthonormality conditions are applied to the above equation, a set of n uncoupled differential equations of the following form result:

$$\dot{\eta}_i(t) - \lambda_i \, \eta_i(t) = \psi_{Li}^T \; F \tag{A.33}$$

Before leaving the topic of adjoint eigenproblems, one additional point will be made. If the A and B matrices in Eqs. (A.13) and (A.14) are symmetric, then the left (adjoint) and right (standard) eigenvectors are clearly identical. This is interesting in view of the fact that the differential equation from which the eigenproblems originated is non-self-adjoint. (See Eqs. (A.9) and (A.10)). This fact is very useful if residual attachment modes are to be employed, since their

calculation involves a knowledge of both left and right-hand eigen-vectors.

3.   Variational Principles

A brief outline of variational principles and some of their uses will now be presented. The discussion is not intended to be an in-depth development of variational principles, but is rather aimed at giving the unfamiliar reader a reasonable background for understanding the body of this thesis and from which more rigorous presentations can be evolved (Ref. 9).

For practical purposes, the key to finding a variational principle for a particular problem is the identification of the correct functional. The functional is a scalar quantity, usually expressed as an integral, whose conditions for stationarity are the governing equations for the problem. The stationarity conditions are commonly referred to as the "Euler equations."

The field of structural mechanics provides the following simple, yet very powerful example of a variational principle. If the functional is written in terms of displacement variables and is equated with the total potential energy of the structural system, then the Euler equations corresponding to this functional are simply the equi-librium equations of the structure. This "variational procedure" is identical to the concept of minimum potential energy at equilibrium.

A problem of great interest as far as the coupling procedure is concerned can be stated as follows: Given the governing differential equations, find the functional whose Euler equations reproduce the given differential equations. As one might expect, the form of the

functional is dependent upon whether or not the differential equation is self-adjoint or non-self-adjoint.

If the differential equation is written as

$$\underset{\approx}{L}(\underset{\sim}{x}) = \underset{\sim}{F} \qquad (A.34)$$

and $\underset{\approx}{L}$ is a self-adjoint operator, then the functional whose Euler equation is Eq. (A.34) is

$$\pi = \int_0^t (\frac{1}{2} \underset{\sim}{x}^T \underset{\approx}{L}(\underset{\sim}{x}) - \underset{\sim}{x}^T \underset{\sim}{F}) \, dt \qquad (A.35)$$

As an example, it will be shown that for the following self-adjoint equation:

$$\underset{\approx}{M}\underset{\sim}{\ddot{x}} + \underset{\approx}{K}\underset{\sim}{x} = \underset{\sim}{F} \qquad (A.36)$$

where $\underset{\approx}{M}$ and $\underset{\approx}{K}$ are symmetric, Eq. (A.35) provides the correct functional.

Upon substitution of Eq. (A.36) into Eq. (A.35), it is seen that the functional takes the form

$$\pi = \int_0^t (\frac{1}{2} \underset{\sim}{x}^T [\underset{\approx}{M}\underset{\sim}{\ddot{x}} + \underset{\approx}{K}\underset{\sim}{x}] - \underset{\sim}{x}^T \underset{\sim}{F}) \, dt \qquad (A.37)$$

The Euler equation is obtained by setting the first variation of equal to zero, i.e.

$$\delta\pi = 0 \qquad (A.38)$$

Application of Eq. (A.38) to Eq. (A.37) results in

$$\int_0^t \left(\frac{1}{2} \delta \underset{\sim}{x}^T [M \underset{\approx}{\ddot{x}} + K \underset{\approx}{x}] + \frac{1}{2} \underset{\sim}{x}^T [M \delta \underset{\approx}{\ddot{x}} + K \delta \underset{\approx}{x}] - \delta \underset{\sim}{x}^T \underset{\sim}{F}\right) dt = 0 \quad (A.39)$$

After the middle term is integrated by parts, the following expression is obtained:

$$\left[\underset{\sim}{x}^T \underset{\approx}{M} \delta \underset{\sim}{\dot{x}} - \underset{\sim}{\dot{x}}^T \underset{\approx}{M} \delta x\right]_0^t + \int_0^t \delta \underset{\sim}{x}^T (M \underset{\approx}{\ddot{x}} + K \underset{\approx}{x} - \underset{\sim}{F}) \, dt = 0 \quad (A.40)$$

Since $\delta \underset{\sim}{x}^T$ is arbitrary, the following condition must exist for the above equation to be satisfied:

$$M \underset{\approx}{\ddot{x}} + K \underset{\approx}{x} - \underset{\sim}{F} = \underset{\sim}{0} \quad (A.41)$$

which is, of course, the equation we started with.

A very useful property of the variational form of the differential equation is the way that approximations are handled in a natural manner. For example, if Eq. (A.36) is to be solved subject to the following Ritz vector approximation:

$$\underset{\sim}{x} = \underset{\approx}{\Phi} \underset{\sim}{\eta}(t) \quad (A.42)$$

then this approximation should be substituted into the variational form of the differential equation (Eq. (A.39)). This substitution leads to

$$\int_0^t \left(\frac{1}{2} \delta \underset{\sim}{\eta}^T \underset{\approx}{\Phi}^T [M \underset{\approx}{\Phi} \underset{\sim}{\eta} + K \underset{\approx}{\Phi} \underset{\sim}{\eta}] + \underset{\sim}{\eta}^T \underset{\approx}{\Phi}^T [M \underset{\approx}{\Phi} \delta \underset{\sim}{\eta} + K \underset{\approx}{\Phi} \delta \underset{\sim}{\eta}] \right.$$

$$\left. - \delta \underset{\sim}{\eta}^T \underset{\approx}{\Phi}^T \underset{\sim}{F}\right) dt = 0 \quad (A.43)$$

Upon integration by parts, the above equation is reduced to

$$[\underset{\sim}{\eta}^T \underset{\approx}{\Phi}^T M \underset{\approx}{\Phi} \delta \dot{\underset{\sim}{\eta}} - \dot{\underset{\sim}{\eta}}^T \underset{\approx}{\Phi}^T M \underset{\approx}{\Phi} \delta \underset{\sim}{\eta}]_0^t +$$

$$\int_0^t \delta \underset{\sim}{\eta}^T (\underset{\approx}{\Phi}^T M \underset{\approx}{\Phi} \ddot{\underset{\sim}{\eta}} + \underset{\approx}{\Phi}^T K \underset{\approx}{\Phi} \underset{\sim}{\eta} - \underset{\approx}{\Phi}^T \underset{\sim}{F}) \, dt = 0 \qquad (A.44)$$

Clearly, for the above expression to be satisfied for all the following must be true:

$$\underset{\approx}{\Phi}^T M \underset{\approx}{\Phi} \ddot{\underset{\sim}{\eta}} + \underset{\approx}{\Phi}^T K \underset{\approx}{\Phi} \underset{\sim}{\eta} - \underset{\approx}{\Phi}^T \underset{\sim}{F} = \underset{\sim}{0} \qquad (A.45)$$

The above equation is simply the form of the original differential equation subjected to the Ritz approximation.

An important point to consider is the case where the differential equation represented by Eq. (A.34) is non-self-adjoint. In this case the functional takes the form (Ref. 9)

$$\pi \quad \int_0^t (\underset{\sim}{y}^T \underset{\approx}{L}(\underset{\sim}{x}) - \underset{\sim}{F}^T \underset{\sim}{y} - \underset{\sim}{F}^{*T} \underset{\sim}{x}) \, dt \qquad (A.46)$$

where $\underset{\sim}{y}$ is the adjoint displacement vector, and $\underset{\sim}{F}^*$ is the adjoint force vector. As will be shown by example, the functional in Eq. (A.46) produces two matrix Euler equations. One is the original differential equation, and the second is the adjoint differential equation.

These properties will be demonstrated in the following example:

$$\underset{\approx}{A}\dot{\underset{\sim}{x}} + \underset{\approx}{B}\underset{\sim}{x} = \underset{\sim}{F} \qquad (A.47)$$

The functional for this problem is seen to be

$$\pi = \int_0^t (\underset{\sim}{y}^T [\underset{\approx}{A}\dot{\underset{\sim}{x}} + \underset{\approx}{B}\underset{\sim}{x}] - \underset{\sim}{F}^T \underset{\sim}{y} - \underset{\sim}{F}^{*T} \underset{\sim}{x}) \ dt \qquad (A.48)$$

Setting the variation of π equal to zero leads to

$$\pi = \int_0^t (\delta\underset{\sim}{y}^T[\underset{\approx}{A}\dot{\underset{\sim}{x}} + \underset{\approx}{B}\underset{\sim}{x}] + \underset{\sim}{y}^T[\underset{\approx}{A}\delta\dot{\underset{\sim}{x}} + \underset{\approx}{B}\delta\underset{\sim}{x}] - \underset{\sim}{F}^T\delta\underset{\sim}{y} - \underset{\sim}{F}^{*T}\delta\underset{\sim}{x}) \ dt \ = \ 0 \qquad (A.49)$$

Integrating the second term by parts yields

$$[\underset{\sim}{y}^T \underset{\approx}{A} \delta\underset{\sim}{x}]_0^t \ + \ \int_0^t (\delta\underset{\sim}{y}^T[\underset{\approx}{A}\dot{\underset{\sim}{x}} + \underset{\approx}{B}\underset{\sim}{x} - \underset{\sim}{F}]$$

$$+ \ \delta\underset{\sim}{x}^T[-\underset{\approx}{A}^T\dot{\underset{\sim}{y}} + \underset{\approx}{B}^T\underset{\sim}{y} - \underset{\sim}{F}^*]) \ dt \ = \ 0$$

Since $\delta\underset{\sim}{y}$ and $\delta\underset{\sim}{x}$ are arbitrary, the Euler equations for the functional in Eq. (A.48) are

$$\underset{\approx}{A}\dot{\underset{\sim}{x}} + \underset{\approx}{B}\underset{\sim}{x} - \underset{\sim}{F} \ = \ \underset{\sim}{0} \qquad (A.50)$$

$$-\underset{\approx}{A}^T\dot{\underset{\sim}{y}} + \underset{\approx}{B}^T\underset{\sim}{y} - \underset{\sim}{F}^* \ = \ \underset{\sim}{0} \qquad (A.51)$$

Of course, Eqs. (A.50) and (A.51) are recognized as the original differential equation and its adjoint. Approximate differential equations can be constructed for the non-self-adjoint system in the same manner as for the self-adjoint case.

REFERENCES

1. Bathé, K.J., and Wilson, E.L., <u>Numerical Methods in Finite Element Analysis</u>, Prentice-Hall, Inc., Englewood Cliffs, NJ, 1976.

2. Chung, Y.T., "Application and Experimental Determination of Substructure Coupling For Damped Structural Systems," Ph.D. Dissertation, The University of Texas, Austin, TX, 1982.

3. Chung, Y.T. and Craig, R.R., "State Vector Formulation of Substructure Coupling For Damped Systems," Paper No. 83-0965, <u>AIAA/ASME/ASCE/AHS 24th Structures, Structural Dynamics, and Materials Conference</u>, Lake Tahoe, May, 1983.

4. Craig, R.R., Jr., <u>Structural Dynamics: An Introduction to Computer Methods</u>, John Wiley and Sons, Inc., New York, 1981.

5. Craig, R.R., Jr. and Bampton, M.C.C., "Coupling of Substructures for Dynamic Analysis," <u>AIAA Journal</u>, Vol. 6, No. 7, July, 1968, pp. 1313-1319.

6. Craig, R.R., Jr. and Chang, C.J., "On the Use of Attachment Modes in Substructure Coupling for Dynamic Analysis," Paper No. 77-405, <u>AIAA/ASME/ASCE/AHS 18th Structures, Structural Dynamics and Materials Conference</u>, San Diego, March, 1977, pp. 89-99.

7. Craig, R.R., Jr. and Chang, C.J., "Substructure Coupling For Dynamic Analysis and Testing," NASA CR-2781, Feb., 1977.

8. Duncan, W.J., Collar, A.R., and Frazer, R.A., Elementary Matrices, Macmillan Company, New York, 1946.

9. Finlayson, B.A., The Method of Weighted Residuals and Variational Principles, Academic Press, Inc., New York, 1972.

10. Greenberg, M.D., Foundation of Applied Mathematics, Prentice-Hall, Inc., Englewood Cliffs, New Jersey, 1978.

11. Hale, A.L., "On Substructure Synthesis and Its Iterative Improvement For Large Nonconservative Vibratory Systems," Paper No. 82-0772, AIAA/ASME/ASCE/AHS 23rd Structures, Structural Dynamics, and Materials Conference, New Orleans, May, 1982, pp. 582-593.

12. Hale, A.L. and Bergman, L.A., "The Dynamic Synthesis of General Nonconservative Structures From Separately Identified Substructure Models," Paper No. 83-0879, AIAA/ASME/ASCE/AHS 24th Structures, Structural Dynamics, and Materials Conference, Lake Tahoe, May, 1983.

13. Hale, A.L. and Meirovitch, L., "A General Substructure Synthesis Method for the Dynamic Simulation of Complex Structures," Journal of Sound and Vibration, Vol. 69, 1980, pp. 309-326.

14. Hasselman, T.K. and Kaplan, A., "Dynamic Analysis of Large Systems by Complex Modes Synthesis," Journal of Dynamic Systems, Measurement, and Control, Trans. ASME, Vol. 96, Ser. G, Sept., 1974, pp. 327-333.

15. Hintz, R.M., "Analytical Methods in Component Modal Synthesis," AIAA Journal, Vol. 13, No. 8, Aug., 1975, pp. 1007-1016.

16. Hughes, T.J.R., Hilber, H.M., and Taylor, R.L., "A Reduction Scheme For Problems of Structural Dynamics," International Journal of Solids and Structures, Vol. 12, 1976, pp. 749-767.

17. Hurty, W.C., "Dynamic Analysis of Structural Systems Using Component Modes," AIAA Journal, Vol. 3, No. 4, April, 1965, pp. 678-685.

18. Meirovitch, L., Computational Methods in Structural Dynamics, Sijthoff-Noordhoff International Publishers, Alphen ann den Rijn, The Netherlands, 1980.

19. Meirovitch, L. and Hale, A.L., "A General Dynamic Synthesis For Structures with Discrete Substructures," Paper No. 80-0798, AIAA/ASME/ASCE/AHS 21st Structures, Structural Dynamics, and Materials Conference, Seattle, May, 1980, pp. 790-800.

20. Meirovitch, L. and Hale, A.L., "On the Substructure Synthesis Method," AIAA Journal, Vol. 19, No. 7, July, 1981, pp. 940-947.

21. MSC/NASTRAN, Handbook for Dynamic Analysis, ed. M.A. Gockel, MSC/NASTRAN Version 63, The MacNeal-Schwendler Corp., Los Angeles, June, 1983.

22. Rubin, S., "Improved Component-Mode Representation for Structural Dynamic Analysis," AIAA Journal, Vol. 13, No. 8, Aug., 1975, pp. 995-1006.

23. Shilov, G.E., Linear Algebra, Dover Publications, Inc., New York, 1977.

24. Wilkinson, J.H., The Algebraic Eigenvalue Problem, Oxford University Press, London, 1965.

25. Wilson, E.L., Yuan, M.W., Dicken, J.M., "Dynamic Analysis By Direct Superposition of Ritz Vectors," Earthquake Engineering and Structure Dynamics, Vol. 10, 1982, pp. 813-821.

26. Zienkiewicz, O.C., The Finite Element Method, McGraw-Hill Book Company (UK) Limited, London, 1977.